



Pacific Northwest
NATIONAL LABORATORY

*Proudly Operated by **Battelle** Since 1965*

Behind the Meter Grid Services: Intelligent Load Control

November 2016

W Kim
S Katipamula
RG Lutes
RM Underhill

DISCLAIMER

This report was prepared as an account of work sponsored by an agency of the United States Government. Neither the United States Government nor any agency thereof, nor Battelle Memorial Institute, nor any of their employees, makes **any warranty, express or implied, or assumes any legal liability or responsibility for the accuracy, completeness, or usefulness of any information, apparatus, product, or process disclosed, or represents that its use would not infringe privately owned rights.** Reference herein to any specific commercial product, process, or service by trade name, trademark, manufacturer, or otherwise does not necessarily constitute or imply its endorsement, recommendation, or favoring by the United States Government or any agency thereof, or Battelle Memorial Institute. The views and opinions of authors expressed herein do not necessarily state or reflect those of the United States Government or any agency thereof.

PACIFIC NORTHWEST NATIONAL LABORATORY
operated by
BATTELLE
for the
UNITED STATES DEPARTMENT OF ENERGY
under Contract DE-AC05-76RL01830

Printed in the United States of America

Available to DOE and DOE contractors from the
Office of Scientific and Technical Information,
P.O. Box 62, Oak Ridge, TN 37831-0062;
ph: (865) 576-8401
fax: (865) 576-5728
email: reports@adonis.osti.gov

Available to the public from the National Technical Information Service
5301 Shawnee Rd., Alexandria, VA 22312
ph: (800) 553-NTIS (6847)
email: orders@ntis.gov <<http://www.ntis.gov/about/form.aspx>>
Online ordering: <http://www.ntis.gov>



This document was printed on recycled paper.

(8/2010)

Behind the Meter Grid Services: Intelligent Load Control

WH Kim
S Katipamula
RG Lutes
RM Underhill

September 2016

Prepared for
the U.S. Department of Energy
under Contract DE-AC05-76RL01830

Pacific Northwest National Laboratory
Richland, Washington 99352

Summary

This report describes how the intelligent load control (ILC) algorithm can be implemented to achieve peak demand reduction while minimizing impacts on occupant comfort. The algorithm was designed to minimize the additional sensors and minimum configuration requirements to enable a scalable and cost-effective implementation for both large and small-/medium-sized commercial buildings. The ILC algorithm uses an analytic hierarchy process (AHP) to dynamically prioritize the available curtailable loads based on both quantitative (deviation of zone conditions from set point) and qualitative rules (types of zone). Although the ILC algorithm described in this report was highly tailored to work with rooftop units, it can be generalized for application to other building loads such as variable-air-volume (VAV) boxes and lighting systems.

As renewable generation technologies form a significant (>20%) fraction of grid capacity, utilities will be forced to maintain a significant standby capacity to mitigate the imbalance between supply and demand because the generation remains variable in nature. Because buildings consume more than 75% of electricity, building loads can be used to mitigate some of the imbalance. This report describes Pacific Northwest National Laboratory's (PNNL's) design, development, testing, and validation of the ILC algorithm that can be used to manage loads in a building or group of buildings using both quantitative and qualitative criteria. It describes how the ILC algorithm can be implemented to achieve peak demand reduction while minimizing impacts on occupant comfort.

The ILC algorithm can be implemented on low-cost single-board computers (Raspberry PI, BeagleBone, etc.). By anticipating future demand, the ILC process can be extended to add advanced control features such as precooling and preheating to alleviate comfort issues when operation of the rooftop units is curtailed to manage the peak demand.

The ILC algorithm was initially tested in a simulation environment to control a group of rooftop units to manage the building's peak demand while still keeping zone temperatures within acceptable deviations. After successful testing of the algorithm in the simulation environment, it was successfully deployed on a building on the PNNL campus in Richland, Washington. The test demonstrated how the ILC algorithm could be used to maintain the target peak while maintaining satisfactory comfort.

Acknowledgments

The authors acknowledge the Buildings Technologies Office of the U.S. Department of Energy Office of Energy Efficiency and Renewable Energy for supporting the research and development effort. The authors would also like to acknowledge valuable guidance from Mr. George Hernandez and Mr. Joseph Hagerman and also thanks Dr. Marina Sofos.

Acronyms and Abbreviations

A_{normal}	normalized criteria judgment matrix
A_p	principal eigenvector
a_{ij}	entry of criteria judgment matrix
AHP	analytic hierarchy process
B	normalized alternative decision matrix
b	entry of alternative decision matrix
C	decision priority vector
c	entry of decision priority vector
CR	Consistency Ratio
Cooling	cooling mode
CI	Consistency Index
$C_{z,eff}$	effective zone thermal capacitance
EMA	exponential moving average
°F	degree(s) Fahrenheit
ft	foot (feet)
HP	heat pump
IB	intelligent building
kW	kilowatt(s)

Abbreviations

A	judgment matrix
A_{normal}	normalized criteria judgment matrix
A_p	principal eigenvector
a_{ij}	entry of criteria judgment matrix
AHP	analytic hierarchy process
B	normalized alternative decision matrix
b	entry of alternative decision matrix
C	decision priority vector
c	entry of decision priority vector
CR	Consistency Ratio
Cooling	cooling mode
CI	Consistency Index
$C_{z,eff}$	effective zone thermal capacitance
EMA	exponential moving average

<i>Heating</i>	heating mode
<i>ILC</i>	intelligent load control
n_{rtu}	number of RTU curtailing
P_{rated}	rated RTU power consumption
P_{peak}	target electric power consumption
$Power_{rtu}$	RTU power consumption
Q_b	rate of instantaneous heat gain to the building air
Q_c	sensible cooling load
RI	random index of consistency
$Room_{rtu}$	room priority
$RTUs$	rooftop units
RTU_{stg}	RTU stage
$s(t)$	binary signal
T_{sp}	set point temperature
T_{zone}	zone temperature measurement
ΔT_{zone_csp}	temperature difference between zone and zone cooling set point
ΔT_{zone_hsp}	temperature difference between zone and zone heating set point
$\Delta T_{zone_}\delta$	zone temperature difference
t	current time
$t-\delta$	previous sampling time
Δt	sampling period
V	raw summation of alternative judgment matrix
v_i	element of raw summation of alternative judgment matrix
W	column summation of criteria judgment matrix
w_i	element of column summation of criteria judgment matrix
WBE	whole building energy

Subscripts

I	<i>raw element of matrix</i>
J	column element of matrix
n	raw number of matrix
m	column number of matrix
$t-\delta$	previous reading

Greek

δ	<i>sampling period</i>
λ	eigenvalue

λ_{max}

maximum eigenvalue

\vec{v}

eigenvector

Contents

Summary	iii
Acknowledgments.....	v
Acronyms and Abbreviations	vii
1.0 Introduction	1
2.0 Description of the Analytic Hierarchy Process.....	3
2.1 Pair-Wise Comparison of Selected Criteria	3
2.2 Formulation of the Priority Criteria Vector.....	3
2.3 Consistency Checking.....	4
2.4 Aggregation of Final Priorities.....	5
3.0 Load Forecasting to Establish Target Peak Demand	6
4.0 Intelligent Load Control Using AHP	8
4.1 Prioritization Criteria.....	8
4.1.1 Criterion 1: RTU Power Consumption.....	8
4.1.2 Criterion 2: Number of RTU Curtailments	8
4.1.3 Criterion 3: Rate of Change in Zone Temperature.....	8
4.1.4 Criterion 4: Deviation of Zone Temperature from Zone Set Point	9
4.1.5 Criterion 5: Room/Zone Type	10
4.1.6 Criterion 6: Cooling/Heating Stage.....	10
4.2 Additional Control Inputs for Load Curtailment.....	11
4.2.1 Temperature Offset Value	11
4.2.2 Curtailment Time Period.....	11
4.2.3 Target Peak Demand	11
4.2.4 Minimum RTU Runtime	12
4.2.5 RTU Operating Mode (Heating or Cooling).....	12
4.2.6 Maximum Curtailed Number	12
5.0 Intelligent Load Control Process	13
5.1 Preprocessing Based on Exponential Moving Average Method.....	13
5.2 RTU Prioritization Based on AHP.....	14
5.2.1 Evaluation of Each Criterion.....	14
5.2.2 Calculation of Criteria Priority Vector.....	15
5.2.3 Calculation of Alternative Matrix	15
5.2.4 Calculation of Decision Priority Vector.....	16
5.2.5 Load Control Based on the Decision Priority Vectors.....	16
6.0 Simulation Results and Discussion.....	18
6.1 Case Study: Analysis and Validation of Intelligent Load Curtailment with Different Curtailment Time Periods	19

6.1.1	Case Study: Analysis and Validation of Intelligent Load Curtailment with Different Target Peak Demand Values	24
7.0	Discussion of Field Test Results	27
7.1	Field Test Results for ILC	28
7.1.1	Field Test Results for ILC during the Heating Season.....	28
7.1.2	Field Test Results for ILC during the Cooling Season (July)	31
7.1.3	Demonstration Results for ILC during the Cooling Season (August).....	34
8.0	Conclusions	38
9.0	References	39

Figures

Figure 1. Comparison between the actual and predicted demand for the building on the PNNL campus....	7
Figure 2. Example of zone and set point temperature at each sampling period in cooling mode.....	9
Figure 3. AHP model for managing building peak demand using RTU loads	13
Figure 4. Example of pair-wise comparison of ILC decision criteria.....	14
Figure 5. Electricity consumption profile under different ILC time periods	20
Figure 6. Weekly electricity consumption profiles under different ILC time periods	21
Figure 7. Zone temperature profiles for different ILC time periods	22
Figure 8. Electric demands under different target peak demand values	24
Figure 9. Zone temperature profile under different target peak demand values	25
Figure 10. External view of the building on PNNL campus.....	27
Figure 11. Location of heat pump in the building on the PNNL campus	27
Figure 12. Electric demand and outdoor temperature profiles during the heating season	29
Figure 13. Example of temperature and heat pump status signal profiles during ILC (March15)	30
Figure 14. Electric demand and outdoor temperature profiles during cooling season.....	32
Figure 15. Example of temperature and heat pump stage profiles the at the test building during ILC	33
Figure 16. Electric demand and outdoor temperature profiles during cooling season at the test building	35
Figure 17. Temperature and heat pump status signal profiles at the test building during ILC	36

Tables

Table 1. Ranking scale for criteria (Saaty and Vargas 2013).	3
Table 2. Random index table (Saaty and Vargas 2013).....	5
Table 3. Example of AHP priority based on room type.....	10
Table 4. Example of stage priority based on cooling/heating stages.	11
Table 5. Example of normalized judgment matrix and eigenvector of criteria.....	15
Table 6. Example of RTU input data for the alternative decision matrix	15
Table 7. Example of the alternative decision matrix of RTUs.....	16
Table 8. Example of the decision priority vector for load curtailment	16
Table 9. Example of RTU set points based on the decision priority vector.....	17
Table 10. Major building simulation parameters.	18
Table 11. Comparison of zone temperatures under different ILC time periods	23
Table 12. RTU ON-OFF cycles and run times under different ILC time periods	23
Table 13. Comparison of zone temperatures under different target peak demand	26
Table 14. RTU ON-OFF cycles and runtime under different target peak demand values.....	26
Table 15. Details of the heat pumps.....	28
Table 16. Summary of curtailment of each heat pump during ILC (March 15)	31
Table 17. Summary of curtailment of each heat pump for the cooling case study	34
Table 18. Summary of curtailment of each heat pump for the cooling case study	37

1.0 Introduction

To mitigate the impacts of climate change, there is a significant impetus to make generation of electricity in the United States cleaner by installing rooftop solar photovoltaic and utility-scale wind generation systems. Although these renewable energy generation technologies are cleaner, their generation of electricity is variable in nature. As these technologies form a significant (>20%) fraction of the grid capacity, utilities will be forced to maintain a significant standby capacity to mitigate the imbalances between supply and demand. The traditional approach of balancing power is cost-effective when the utilities only had to maintain between 5% and 10% of the capacity. An alternative approach to mitigating this imbalance is to manage the load (demand side). Because more than 75% of electricity consumption occurs in buildings, building loads can be used to mitigate some of the imbalance.

The control of building end-use loads has been shown to provide significant demand relief in response to grid needs (Lu and Katipamula 2005). In addition, building loads have been used to limit electric demand when a demand charge is a significant percentage of the total energy cost or when a building has to maintain a certain level of maximum demand in response to changes in the price of electricity over time. However, an accurate and reliable load control strategy is required to manage peak loads because even one excursion could cause a significant increase in utility bills.

The duty-cycling control strategy has been traditionally used to manage peak demand by controlling the ratio of the ON-period to the total cycle time of rooftop units (RTUs) or air-handling units (Krarti 2000). Two traditional duty-cycling strategies exist for operating building RTUs (Thumann and Mehta 2001): 1) a parallel duty-cycling approach, in which all RTUs are cycled ON or OFF at the same time; and 2) a staggered duty-cycling approach, in which the RTU ON and OFF cycles are staggered. For example, in the case of staggered duty-cycling only, some (e.g., 1/3 or 2/3) of the RTUs operate at any given time. Although both duty-cycling methods provide relief from electric demand, neither dynamically prioritizes the RTUs' operation to be curtailed to manage peak electricity consumption. It is generally difficult to identify the RTUs whose operations can be curtailed without affecting zone comfort, and indiscriminate curtailment of RTUs can lead to comfort issues by negatively affecting the zone temperature and humidity conditions. Therefore, a load control strategy is needed that anticipates the future effects of thermal comfort and peak load relief based on current conditions and historical data.

This report describes Pacific Northwest National Laboratory's (PNNL's) development and validation of one such intelligent load control (ILC) algorithm that can be used to manage load while also considering occupant comfort. The ILC algorithm can dynamically prioritize the available loads for curtailment using both quantitative (deviation of zone conditions from set point) and qualitative rules (type of zone) in a building or multiple buildings (a campus). The ILC algorithm uses the analytic hierarchy process (AHP) to prioritize loads for curtailment.

The AHP is a structured technique for organizing and analyzing complex decisions based on mathematics and psychology (Saaty and Vargas 2013). The process can generate a numerical score to establish the prioritization of each alternative being considered based on associated decision criteria. The AHP is applicable when it is difficult to formulate a goal or quantitative criteria for evaluation. The AHP also allows for the use of qualitative as well as quantitative criteria to solve complex decision-making problems (Cheng and Li 2002). It decomposes the problems into a hierarchy of elements influencing a system by incorporating three levels: the *objectives*, *criteria*, and *alternatives of a decision*. The process has the ability to prioritize a set of criteria used to rank the alternatives of a decision and distinguish, in general, the more important factors from the less important factors. Pair-wise comparison judgments are made with respect to the attributes of one level of hierarchy given the attribute of the next higher level of

hierarchy from the main criteria to the sub-criteria (Crowe and Noble 1998). AHP can also solicit consistent subjective expert judgment by using a consistency test. Triantaphyllou and Stuart (1995) applied the AHP to solving complex multi-criteria decision-making problems in a matrix structure.

The AHP method has been used for demand response control in the power sector. Ding et al. (2006) proposed a dynamic load-shedding scheme of electric power systems based on the AHP decision-making process. According to Aalami et al. (2010), the AHP can be used to deal with multiple market operational problems such as price spikes, insufficient spinning reserve margin, and system security and reliability. Goh and Kok (2010) discussed the AHP applied to similar dynamic load-shedding operational problems for the electrical power system. They prioritized dynamic loads according to their importance by using criteria determined from previous experiences and case studies.

Only a few studies used AHP for building applications. Yao et al. (2004) applied the AHP to integrate the advantages of four forecasting models of cooling loads and improved accuracies. In that case, the AHP was employed to determine the optimal weights of each model. The proposed approach was shown to significantly improve cooling load forecasting by using pair-wise judgments between models with periodically updated weights. The research conducted by Wong and Li (2008) proposed a multi-criteria decision-making model using the AHP to evaluate the selection of intelligent building (IB) systems. They identified key selection criteria for IB systems based on a survey of IB practitioners. The AHP was applied to prioritize and assign important weights to the perceived criteria in the survey. The results suggest that the IB system was determined by a disparate set of selection criteria that had different weightings. Work efficiency is perceived to be the most important core selection criterion for various IB systems; user comfort, safety, and cost-effectiveness are also considered significant. Bian et al. (2015) introduced an expert-based demand curtailment allocation approach using the AHP, which allowed an electric utility to prioritize the load curtailment for each of its distribution substations using load levels, capacity, customer types, and load categories. The AHP was used to model a decision-making process according to opinions from experts and objective parameters. Simulation case studies were performed to show the demand curtailment allocations among different distribution substations.

This report describes a load control strategy based on a dynamic prioritization of a list of curtailable loads (e.g., RTUs) that is updated frequently. The ILC based on the AHP was first evaluated and validated using a simulation model that employs four RTUs. Simulation studies were performed to demonstrate how the ILC algorithm can be implemented to manage peak energy consumption. Simulation results showed that ILC algorithm is capable of reducing peak demand without significantly reducing occupant comfort. Overall, the ILC algorithm allows coordination of the RTU operations and provides more intelligent means of load management than the traditional duty-cycling approach.

2.0 Description of the Analytic Hierarchy Process

The AHP is a structured technique for organizing and analyzing complex decisions. It provides the capability to specify numerical weights representing the relative importance of each individual alternative as well as their associated criteria with respect to the goal. The AHP consists of four steps: 1) pair-wise comparison of selected criteria, 2) formulation of a priority criteria vector, 3) consistency checking, and 4) aggregation of final priorities. Each of these four steps is briefly described below followed by a detailed description of an example implementation.

2.1 Pair-Wise Comparison of Selected Criteria

The AHP was developed based on the calculation of eigenvector, \vec{v} , between a pair of alternatives under evaluation (Saaty 2003). The $A(\vec{v})$ can be calculated by multiplying the eigenvalue, λ , corresponding to \vec{v} as shown in Equation (1).

$$A(\vec{v}) = \lambda \cdot \vec{v} \quad (1)$$

The λ indicates the comparison rank of criteria, which has ranking values between 1/9 and 9 that are given by the decision-makers. The relative importance of the two criteria is measured and evaluated according to a numerical scale from 1 to 9. **Error! Reference source not found.** shows how to translate the decision-maker's qualitative evaluations of the relative importance of the two criteria into numbers. It is also possible to assign intermediate values (e.g., 2, 4, 6, and 8) that do not correspond to a precise interpretation. The higher the value, the more important the corresponding criterion is. Pair-wise comparison is conducted to determine qualitatively which criteria are more important and assign to each criterion a qualitative weight. For example, if λ_a is absolutely more important than λ_b it is assigned a value of 9, and λ_b must be absolutely less important than λ_a so it is valued at 1/9.

Table 1. Ranking scale for criteria (Saaty and Vargas 2013).

Intensity of Importance	Definition	Explanation
1	Equal importance	Two criteria contribute equally to the goal.
3	Somewhat more important	One criterion is slightly more important than the other.
5	Much more important	One criterion is strongly more important.
7	Very much more important	One criterion is very strongly more important.
9	Absolutely more important	One criterion is absolutely more important.
2, 4, 6, 8	Intermediate values	These values are used when compromise is needed.

2.2 Formulation of the Priority Criteria Vector

A judgment matrix (A) is created based on the pair-wise comparison as shown in Equation (2). The judgment matrix allows a decision-maker to identify, analyze, and rate the strength of relationships between a set of information. The matrix, A is a $n \times n$ real matrix, where n is the number of criteria.

$$A = \begin{bmatrix} a_{11} & \cdots & a_{1n} \\ \vdots & \ddots & \vdots \\ a_{n1} & \cdots & a_{nn} \end{bmatrix} \quad (2)$$

Each entry a_{ij} of A is formed by comparing the row element a_i with the column element a_j . Each entry a_{ij} of the matrix represents the importance of the i^{th} criterion relative to the j^{th} criterion based on Table 1. If $a_{ij} > 1$, then the i^{th} criterion is more important than the j^{th} criterion; if $a_{ij} < 1$, then the i^{th} criterion is less important than the j^{th} criterion. If two criteria have the same importance, then the entry a_{ij} is 1. An element a_{ii} is equally important when compared to itself; therefore, the main diagonal must be $a_{ii} = 1$ for all i . The entries a_{ij} and a_{ji} satisfy Equation (3):

$$a_{ij} \cdot a_{ji} = 1 \quad (3)$$

The matrix, A is normalized by multiplying the inverse of each column summation (W) as shown in Equations (4) and (5). The normalized judgment matrix (A_{normal}) identifies the weights of each criterion. After normalizing, the principal eigenvector (A_p) can be calculated by averaging across the rows shown in Equation (6). The A_p of the criteria is a ratio of the numerical values of the criteria that indicates an order of importance among the different criteria.

$$W = \sum_{j=1}^n a_{ij} = [w_1 \quad \cdots \quad w_n] \quad (4)$$

$$A_{normal} = \begin{bmatrix} \frac{a_{11}}{w_1} & \cdots & \frac{a_{1n}}{w_n} \\ \vdots & \ddots & \vdots \\ \frac{a_{n1}}{w_1} & \cdots & \frac{a_{nn}}{w_n} \end{bmatrix} \quad (5)$$

$$A_p = \begin{bmatrix} \frac{1}{n} \cdot \sum_{j=1}^n \frac{a_{1j}}{w_j} \\ \vdots \\ \frac{1}{n} \cdot \sum_{j=1}^n \frac{a_{nj}}{w_n} \end{bmatrix} \quad (6)$$

2.3 Consistency Checking

Human comparisons can be inaccurate and lead to inconsistency between pair-wise comparisons. A typical example of inconsistency in a pair-wise comparison is as follows: if criterion A has double the importance of criterion B, and criterion B has triple the importance of criteria C, then criterion A should have six times the importance of criteria C. However, if criterion A is determined to have only 4 times the importance of criterion B, this selection will lead to inconsistency. This inconsistency can lead to incorrect decisions. Therefore, Saaty and Vargas (2013) created a consistency test that can be performed by measuring the consistency ratio (CR) using the consistency index (CI) as shown in Equation (7). Table 2 shows the random index (RI) of consistency for varying sizes of matrices. This approach estimates CR to evaluate the degree of inconsistency. If the CR of the matrix is less than 0.2, the pair-wise comparison

is considered consistent. Otherwise, a new comparison matrix needs to be reconstructed for the pair-wise comparisons to meet the desired consistency, thereby leading to optimal decision-making.

$$CR = \frac{CI}{RI} = \frac{\left(\frac{\lambda_{max} - n}{(n-1)}\right)}{RI} \quad (7)$$

where λ_{max} is the maximum eigenvalue of matrix A , and n is the matrix size.

Table 2. Random index table (Saaty and Vargas 2013).

n	1	2	3	4	5	6	7	8	9	10
Random Index	0	0	0.58	0.90	1.12	1.24	1.32	1.41	1.45	1.49

2.4 Aggregation of Final Priorities

The alternative decision matrix, B , is an $n \times m$ real matrix, where n is the number of criteria and m is the number of alternatives as shown in Equation (8). The matrix B is normalized by multiplying the inverse of each row summation of B as shown in Equations (9) and (10).

$$B = \begin{bmatrix} b_{11} & \cdots & b_{1m} \\ \vdots & \ddots & \vdots \\ b_{n1} & \cdots & b_{nm} \end{bmatrix} \quad (8)$$

$$V = \sum_{i=1}^m b_{ij} = \begin{bmatrix} v_1 \\ \vdots \\ v_n \end{bmatrix} \quad (9)$$

$$B_{normal} = \begin{bmatrix} \frac{b_{11}}{v_1} & \cdots & \frac{b_{1m}}{v_1} \\ \vdots & \ddots & \vdots \\ \frac{b_{n1}}{v_n} & \cdots & \frac{b_{nm}}{v_n} \end{bmatrix} \quad (10)$$

The decision priority vector, C , can be calculated by multiplying each element of the normalized alternative decision matrix (B_{normal}) as shown in Equation **Error! Reference source not found.** Overall, the decision priority represents the ranking of each alternative in achieving the goal.

$$C = (A_p)^T \cdot B_{normal} = \left[\frac{1}{n} \cdot \sum_{j=1}^n \frac{a_{1j}}{w_1} \quad \cdots \quad \frac{1}{n} \cdot \sum_{j=1}^n \frac{a_{nj}}{w_n} \right] \cdot \begin{bmatrix} \frac{b_{11}}{v_1} & \cdots & \frac{b_{1m}}{v_1} \\ \vdots & \ddots & \vdots \\ \frac{b_{n1}}{v_n} & \cdots & \frac{b_{nm}}{v_n} \end{bmatrix} = \begin{bmatrix} c_1 \\ \vdots \\ c_m \end{bmatrix} \quad (11)$$

3.0 Load Forecasting to Establish Target Peak Demand

Under the most common billing rate structure, the utilities charge for peak demand. The demand is usually estimated as the highest rolling average over a prespecified interval (e.g., 15- or 30-minute) in the course of the billing period (e.g. a month). The peak demand usually lasts for a relatively short period of time. For example, when the cooling load requires the RTUs' full capacity in the building, all RTUs may be ON simultaneously to meet the temperature set point. The ILC algorithm enables the equipment in the building to be coordinated and minimize the number of units running concurrently, thereby maintaining the target peak at an optimal level. However, if the target peak level is updated based on a fixed demand level only, the following situation could occur: all available curtailed loads are switched OFF during an event, which is regarded by the system as having a demand close to the maximum demand that could be expected. Furthermore, when the event ends, all curtailed loads are likely to turn ON simultaneously once normal control resumes. This type of peak caused is referred to as a secondary peak in demand (Hoffman 1998). Therefore, it is very important to set the target peak demand at exactly the right level in order to only release the available load curtailed capacity at appropriate times. It will be much more acceptable if the peak demand control system has the built-in capability to automatically adjust the target peak level in a manner that will prevent secondary peaks. The curtailable loads can only influence demand levels over relatively short periods. Hence, the effect is mainly to level out fluctuations in the base load. If one can predict the base electrical load as well as the thermal load into the future over such a time period, one can proactively adjust the target peak demand level to a realistically attainable level, even before that level of demand has actually been reached by the system.

To implement the above strategy, whole building energy (WBE) tool is used for optimal adjustment of the target peak level based on time-series forecasting of the overall load of the building (Katipamula et al. 2003). The WBE method can estimate the expected consumption based on historical data and using bin method. A bin is an interval of values of the outdoor temperature, which explains the variation in energy consumption. The outdoor temperatures are grouped into bins of equal size and then the median of energy consumption data are assigned to each bin defined by the ranges of the outdoor temperature. WBE modeling is implemented using a set of structured query language database queries. The method uses hourly outdoor temperature as the dependent variable and building energy consumption as the independent variable. If the inputs are sub-hourly, they are automatically aggregated to hourly values. Users can define a "baseline" time period over which they wish to create a model predicting energy consumption. The expected energy consumption is computed using future weather forecast. The predicted energy consumption for an hour is the median of all of the values of energy consumption for conditions of outdoor temperature close to that of the actual measured value. Outdoor air temperatures within the bin-size limits of the actual temperature determine whether a stored measurement is sufficiently close to be included in the calculation (e.g., within ± 5 °F). For details about WBE refer to Katipamula et al. (2003).

The capability of the WBE method to predict future demand based on 9 months of hourly baseline energy consumption data is shown in Figure 1. The figure compares the predicted average hourly demand with the actual average hourly demand for the building located on the PNNL campus. It can be shown that whole building electricity consumption based on prediction follows the actual consumption profile closely. The target peak for the ILC can be based on the WBE average demand prediction.

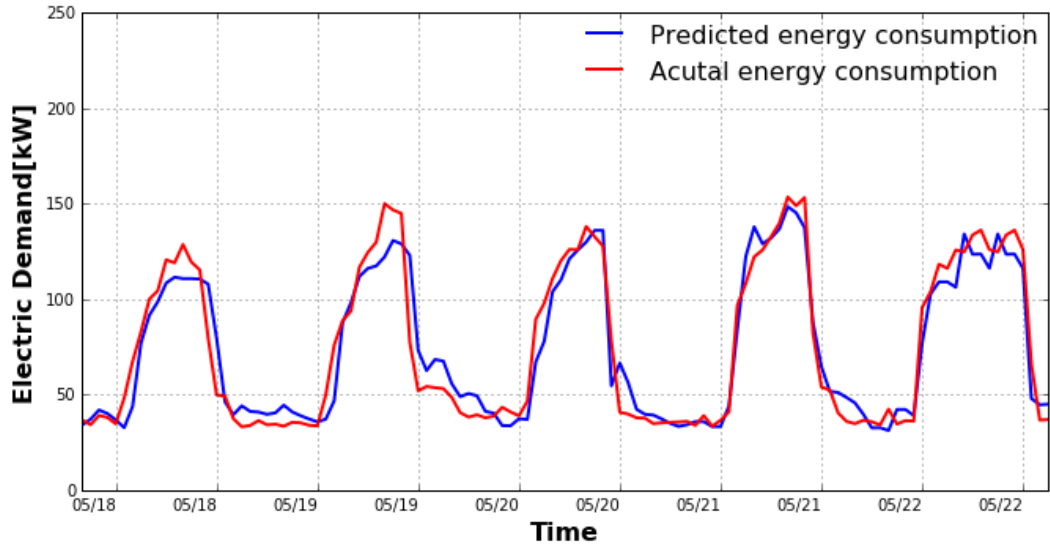


Figure 1. Comparison between the actual and predicted demand for the building on the PNNL campus

4.0 Intelligent Load Control Using AHP

One key aspect of the ILC algorithm is its use of the AHP, which provides a method for prioritizing actions for the best results. AHP strategies can determine whether turning heat pumps OFF or ON in a certain sequence achieves optimum energy savings without harming the comfort of building occupants. The algorithm using AHP can be deployed to manage any homogeneous controllable loads (e.g., a group of RTUs or a group of lighting loads) that have similar inputs and criteria. Heterogeneous loads (e.g., a mixture of RTUs and lighting loads) can also be prioritized, but they have to be separated into homogeneous loads and the AHP applied recursively.

4.1 Prioritization Criteria

Any number of relevant criteria can be used to prioritize loads for curtailment to manage electricity consumption. To illustrate how the ILC process can be used to manage the total RTU energy consumption, six pre-determined criteria are used. Additional criteria can be easily added or existing criteria modified or removed.

4.1.1 Criterion 1: RTU Power Consumption

An estimate or actual measured consumption of the load (RTU) to be controlled is critical to meeting the targeted consumption goal. If measured consumption of the RTU ($Power_{rtu}$) is not available, an estimate based on the rated power consumption can be used. Assuming that the rated power consumption of the RTU is P_{rated} , then the power consumed by RTU, $Power_{rtu}$, is as shown in Equation (11).

$$Power_{rtu} = \begin{cases} P_{rated} & \text{if } s(t) = 1 \\ 0 & \text{if } s(t) = 0 \end{cases} \quad (11)$$

where $s(t) = 0$ implies RTU is OFF and $s(t) = 1$ implies RTU is ON.

4.1.2 Criterion 2: Number of RTU Curtailments

The number of RTU curtailments (n_{rtu}) represents the total number of curtailments an RTU has experienced during a fixed time period, which is typically 24 hours. For any RTU, if the number of curtailments reaches a certain number ($> n_{rtu}$), the corresponding RTU can be excluded from ILC for that day. In general, cycling the RTUs too frequently may result in reduced operating lifespans. This condition may occur when the mass in the zone is small or the RTU is oversized, resulting in a quick change in the zone temperature.

4.1.3 Criterion 3: Rate of Change in Zone Temperature

Zone temperature (T_{zone}) represents the temperature condition of the zone served by an RTU. Differential Equations (12) and (13) describe the separate energy balance for the zone-cooling load, when considering zone temperature transients (Lee and Braun 2008).

$$C_{z,eff} \cdot \frac{\Delta T_{zone_delta}}{\Delta t} = Q_b - Q_c \quad (12)$$

$$\Delta T_{zone_delta} = \frac{(Q_b - Q_c)}{C_{z,eff}} \cdot \Delta t \quad (13)$$

where $C_{z,eff}$ is an effective zone thermal capacitance of the zone air and internal mass, Q_c is the sensible cooling load, and Q_b is the rate of instantaneous heat gain to the building air. Zone temperature difference (ΔT_{zone_delta}) is assumed to vary linearly between the previous sampling time ($t-\delta$) and the time of the last reading (t). If there is no cooling requirement, ΔT_{zone_delta} should be negative for a given time period (Δt).

Figure 2 shows the example of T_{zone} per Δt and zone cooling set point (T_{csp}) in a cooling mode. ΔT_{zone_delta} can be calculated as shown in Equation (14) for the cooling mode and Equation (15) for the heating mode. When the value of ΔT_{zone_delta} is less than or equal to zero, the cooling requirement is less than zero (e.g., RTU turns off) or Q_c is equal to Q_b . Therefore, ΔT_{zone_delta} should be equal to zero.

$$\text{Cooling mode: } \Delta T_{zone_delta} = \begin{cases} (T_{zone,t-\delta} - T_{zone,t}) & \text{if } (T_{zone,t-\delta} - T_{zone,t}) > 0 \\ 0 & \text{if } (T_{zone,t-\delta} - T_{zone,t}) < 0 \end{cases} \quad (14)$$

$$\text{Heating mode: } \Delta T_{zone_delta} = \begin{cases} (T_{zone,t} - T_{zone,t-\delta}) & \text{if } (T_{zone,t} - T_{zone,t-\delta}) > 0 \\ 0 & \text{if } (T_{zone,t} - T_{zone,t-\delta}) < 0 \end{cases} \quad (15)$$

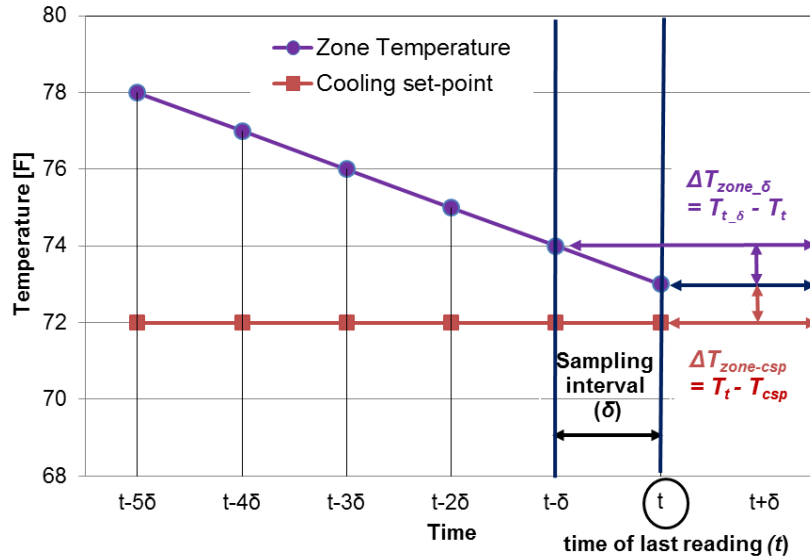


Figure 2. Example of zone and set point temperature at each sampling period in cooling mode.

4.1.4 Criterion 4: Deviation of Zone Temperature from Zone Set Point

The thermostat for the RTU is a feedback controller. The controller relies on a measured zone temperature (T_{zone}), while adjusting the output signals to activate the necessary stages of heating or cooling when the zone is in the occupied mode. In the unoccupied mode, the zone thermostat activates the

necessary stages of cooling or heating, along with the RTU ventilation fan, when the zone temperature rises above the setback upper limit value or falls below the setback lower limit value. The heating set point (T_{hsp}) and T_{csp} represent the zone temperature threshold. The thermostat turns ON the RTU only when the zone temperature is either above the cooling set point or below the heating set point. Once the RTU is turned ON to provide cooling, it remains ON until the zone temperature falls 0.5°F below the set point to protect the RTU from short cycling.

Figure 2 shows an example of temperature difference ($\Delta T_{zone-csp}$) between T_{zone} and T_{csp} in the cooling mode. $\Delta T_{zone-csp}$ reflects the occupant's comfort status in the zone corresponding to each RTU. The input to the AHP is the inverse value of $\Delta T_{zone-csp}$ and $\Delta T_{zone-hsp}$ as shown in Equation (16) for the cooling mode, and Equation (17) for the heating mode, respectively. When the difference between T_{zone} and T_{csp} (or T_{hsp}) is lower than 0.1, $\Delta T_{zone-csp}$ (or $\Delta T_{zone-hsp}$) should be set to 10.

$$\text{Cooling mode: } \Delta T_{zone-csp} = \begin{cases} \frac{1}{(T_{zone} - T_{csp})} & \text{if } (T_{zone} - T_{csp}) > 0.1 \\ 10 & \text{if } (T_{zone} - T_{csp}) \leq 0.1 \end{cases} \quad (16)$$

$$\text{Heating mode: } \Delta T_{zone-hsp} = \begin{cases} \frac{1}{(T_{hsp} - T_{zone})} & \text{if } (T_{hsp} - T_{zone}) > 0.1 \\ 10 & \text{if } (T_{hsp} - T_{zone}) \leq 0.1 \end{cases} \quad (17)$$

4.1.5 Criterion 5: Room/Zone Type

Room priority ($Room_{rtu}$) can be used to prioritize the rooms for curtailment of power consumption. Higher numerical values assigned to a given room is regarded as less important (more likely to be curtailed first) than rooms with lower numerical values. Users would set their own priority depending on the importance of the room (1: most important and 7: less important). Table 3 shows an example of AHP priority based on building room type. The $Room_{rtu}$ weight is zero while heating or cooling operation is OFF. Where an RTU serves multiple spaces of varying importance, users will need to determine the $Room_{rtu}$ as they see fit.

Table 3. Example of AHP priority based on room type.

	Director's Office	Office	Vacated Office	Conference Room	Mechanical Room	Computer Lab	Kitchen
AHP Priority	1	3	7	5	7	1	3

4.1.6 Criterion 6: Cooling/Heating Stage

The modes/stages are allowed to control each RTU. For example, the selection between 1 and 2 is feasible for controlling an RTU with two stages of compressor operation in the cooling mode. The OFF state is denoted as 0. Output stages of 1 and 2 of the RTU indicate the first and second cooling stages of the RTU, respectively. For heating mode, the selection between 1 and 2 is feasible for controlling compressor(s) and electric heater, separately. Second stage cooling would result in peak power consumption but for shorter operating periods, whereas first stage cooling would operate longer with a lower peak power consumption. Second stage heating (electric heater) will also lead to higher peak power consumption with shorter operating periods, than first stage heating (compressor). The ILC algorithm will choose second

stage for load curtailment if it can keep the zone temperature within the comfort band. The stage priority (RTU_{stg}) can be determined using cooling stage and heating stage signals as shown in Table 4.

Table 4. Example of stage priority based on cooling/heating stages.

	First Cooling Stage (1st compressor)	Second Cooling Stage (2nd compressor)	First Heating Stage (Compressor[s])	Second Heating Stage (Electric heater)
Stage Priority (RTU_{stg})	1	3	1	9

4.2 Additional Control Inputs for Load Curtailment

A number of additional parameters, described in the following sections, are needed to prioritize the loads for curtailment.

4.2.1 Temperature Offset Value

If the building electric energy consumption is approaching the targeted peak demand, some or all of the RTUs that are currently running have to be curtailed. In most cases, direct control of the RTUs is not possible; therefore, an alternative approach is used. In the alternative approach, the set points are offset by a fixed value, which will result in the RTU turning OFF. After the event is over or if the next prioritization results in a different set of RTUs on the top, the set points will be restored to normal values. The temperature offset is set to 1°F for the second stage and 2°F for the first stage as default settings. The offset value can be adjusted depending on the cooling/heating load served by each RTU.

4.2.2 Curtailment Time Period

The ILC algorithm manages RTU consumption by cycling the units ON or OFF in a building to prevent the peak demand from exceeding the targeted demand. When the event has ended and the set points for curtailed units are restored to normal, most RTUs are likely to be turned ON. This can result in an unwanted peak demand that can be equal to or even higher than the targeted peak demand value. It is important to manage the targeted peak demand at exactly the right level, in order to release the available loads currently under curtailment at appropriate times. For this reason, the ILC process has an option to specify the curtailment time period. When an RTU is curtailed, it will remain curtailed for the specified duration. The curtailment time period is set to 15-minutes as a default setting. The optimal ILC time period that balances peak demand targets, occupant discomfort, and RTU set point recovery efforts are analyzed in Section 6.2 based on a virtual control test bed.

4.2.3 Target Peak Demand

The building operator can determine the target peak demand, and it can vary hourly, daily, monthly or seasonally. For efficient operation of ILC, it is necessary to accurately model the expected behavior of the sheddable loads. The target peak demand level can be adjusted using the WBE method as previously mentioned in Section 3. The impact of target peak demand is presented in Section 6.2 based on a virtual control test bed.

4.2.4 Minimum RTU Runtime

Cycling the RTU compressor ON or OFF controls RTU operation. Each RTU has a finite lifespan that may be shortened; therefore, RTU manufacturers ensure that the compressors are not cycled frequently. In addition to the safety features built into the RTU, the ILC algorithm ensures that the compressors are not cycled frequently by using a RTU runtime clock. The 5-minute runtime is used as a default. This often means that the RTU is excluded from any priority decision-making until both internal (RTU timers) and external timer values are met.

4.2.5 RTU Operating Mode (Heating or Cooling)

The RTU operating mode represents the heating/cooling status of the RTU. This value is used as a reference input to calculate three criteria values: (1) $RTU_{stg,}$, (2) $\Delta T_{zone-csp}$ or $\Delta T_{zone-hsp}$, and (3) ΔT_{zone_δ} .

4.2.6 Maximum Curtailed Number

Frequent compressor ON/OFF switching can reduce the life of the compressor and deteriorate the performance of the RTU. As the number of curtailments reaches the maximum curtailed number, the corresponding RTU can be excluded from ILC. The maximum curtailed number for a day is set at 50 (per RTU) as a default setting.

5.0 Intelligent Load Control Process

The primary goal of the ILC process is to prioritize controllable loads (e.g., RTUs) that can be curtailed to keep a building's dynamic electric demand from exceeding the targeted demand chosen by the building/facility operations staff. Figure 3 shows that the AHP has three major elements in the decision model: the goal, the criteria, and the alternatives. The AHP comprises relative weights of the decision criteria and the relative priorities of alternatives. The goal of the ILC process is to generate the dynamic load curtailment priority for controlling the building's peak demand to keep from exceeding the target. The intermediate-level consists of five different decision criteria (user selected) as explained below. The lowest level consists of seven different decision alternatives, which are different RTUs that are coordinated to curtail their energy use. Making load curtailment decisions requires comparing alternatives with respect to a set of decision criteria. In this section, an application of the ILC process to manage the peak electricity consumption of a building that has a set of RTUs is explained in detail.

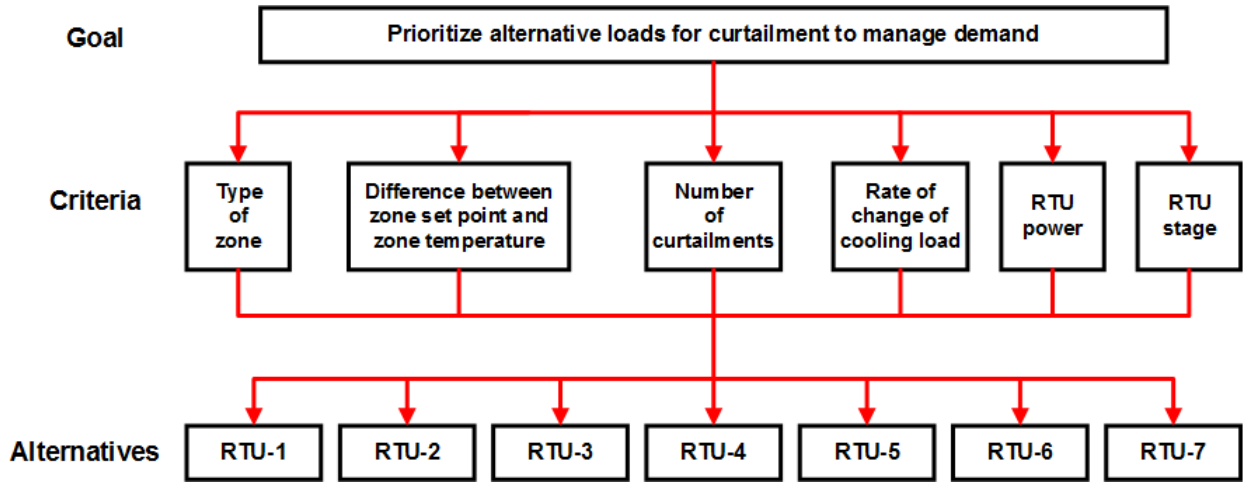


Figure 3. AHP model for managing building peak demand using RTU loads

5.1 Preprocessing Based on Exponential Moving Average Method

The exponential moving average (EMA) method is one of the approaches used for load forecasting, as shown in Equation (18). The widespread use of the EMA method in automated applications, such as inventory control, led Taylor (2003) to consider its use for forecasting online electricity demand. The EMA method is used to predict future demand for ILC input. The EMA differs from a moving average by assigning relatively more weight to most recent observation. It is slightly more responsive to changes occurring in the recent observation. The ILC algorithm can therefore maintain a target level that equals the average predicted total demand level over the specified forecasting window. The value of α is relative to the period for which the forecast is computed as shown in Equation (19). The value of α must be between 0 and 1. A higher value of α is appropriate when the coefficients are shifting rapidly and a lower value when the coefficients are shifting more slowly.

$$F_N = \alpha \cdot D_N + (1 - \alpha) \cdot F_{N-1} = \alpha \cdot D_N + (1 - \alpha) \cdot (\alpha \cdot D_{N-1} + (1 - \alpha) \cdot F_{N-2})$$

$$= \alpha \cdot D_N + (1 - \alpha) \cdot \alpha \cdot D_{N-1} + (1 - \alpha)^2 \cdot \alpha \cdot D_{N-2} + \dots \quad (18)$$

$$\alpha = \frac{2}{(N + 1)} \quad (19)$$

where D_N = new observation or actual value of series,
 F_N = the predicted based load,
 F_{N-1} = last estimate of the observation,
 N = the number of data points, and
 α = smoothing constant for the data.

Before initiating ILC, the following parameters should be determined: 1) current demand estimate based on EMA, 2) target demand level until the end of the demand period, and 3) the demand that could be shed by switching off the RTU(s). The current demand estimate is subtracted from the target peak level to obtain the required demand level to be shed during the remainder of demand period. If the subtracted value is positive, the ILC algorithm will identify RTUs for curtailment based on a priority list allocated to each RTUs. This process will continue either until a sufficient number of RTUs have been selected for achieving the goal, or until all RTUs have been selected for curtailment. For example, the target demand has been selected to be 30 kW, the current demand estimate of RTUs is 36 kW, and the demand to be shed is 6 kW.

5.2 RTU Prioritization Based on AHP

This section describes how the RTU prioritization list is generated.

5.2.1 Evaluation of Each Criterion

Figure 4 shows an example of a pair-wise comparison matrix for the ILC process. The pair-wise comparison is conducted to determine qualitatively which criteria are more important and assign to each criterion a qualitative weight. The defined levels of importance are represented by numbers. Each number represents a different level of importance. For example, if “ ΔT_{zone_d} ” is determined to have greater importance than “ n_{curt} ”, a value of “4” is assigned to this comparison (“x” in a drop-down box between 1 and 9 on the right side). The corresponding reciprocal value is assigned to the reverse comparison between the criteria. Thus, the value of “ n_{curt} ” compared to “ ΔT_{zone_d} ” would be “1/4” to represent its relative importance. Although the table below shows five criteria, additional criteria can be easily added or a criterion can be replaced with another more important one. The ILC deployment includes a template (excel file) for a pair-wise comparison table. The operation staff can change the level of importance of criteria in the pair-wise comparison template (excel file) according to their own preferences. Also, the criteria in the pair-wise comparison template can be replaced or added/updated by a building operator’s selective preferences (e.g., RTU energy efficiency).

Criteria	extreme important		very much important		much important		slightly important		Equal	slightly important		much important		very much important		extreme important		Criteria
	9	8	7	6	5	4	3	2	1	2	3	4	5	6	7	8	9	
Number of RTU curtailed												X						Change of zone temperature
Number of RTU curtailed								X										Room type
Number of RTU curtailed										X								RTU power consumption
Number of RTU curtailed													X					Temperature difference between zone and setpoint
Number of RTU curtailed														X				RTU stages
Change of zone temperature					X													Room type
Change of zone temperature							X											RTU power consumption
Change of zone temperature										X								Temperature difference between zone and setpoint
Change of zone temperature											X							RTU stages
Room type												X						RTU power consumption
Room type																X		Temperature difference between zone and setpoint
Room type															X			RTU stages
RTU power consumption													X					Temperature difference between zone and setpoint
RTU power consumption														X				RTU stages
Temperature difference between zone and setpoint								X										RTU stages

Figure 4. Example of pair-wise comparison of ILC decision criteria

5.2.2 Calculation of Criteria Priority Vector

Table 5 shows the example of matrix A_{normal} and eigenvector A_P of the criteria. The A_{normal} shows the relative weight for each evaluation criterion according to the pair-wise comparisons of the load priority criteria. Because A is normalized by W in Equation (5), the sum of each column in A_{normal} should be 1. The A_P vector shows the ratios of the numerical values that indicate the strength of each criterion's preferences. The priority vector indicates the rankings among the criteria. In Table 5, the most important criterion for prioritizing the curtailable loads is ΔT_{zone_sp} , followed by $\Delta T_{zone_}\delta$, $Power_{rtu}$, n_{rtu} , $Room_{rtu}$, and RTU_{stage} . The priority vector also shows the relative weights of the criteria. ΔT_{zone_sp} is 1.6 times more important than $\Delta T_{zone_}\delta$. The CR value calculated using Equation (7) is 0.04, which is less than 0.1; therefore, the eigenvector A_P of criteria are acceptable.

Table 5. Example of normalized judgment matrix and eigenvector of criteria

Criterion	A_{normal}						A_P
	n_{rtu}	$T_{zone\ at\ t-\delta}$	$T_{zone\ at\ t}$	$Room_{rtu}$	$Power_{rtu}$	RTU_{stage}	
n_{rtu}	0.05	0.04	0.07	0.03	0.07	0.05	0.054
$\Delta T_{zone_}\delta$	0.22	0.15	0.19	0.19	0.15	0.12	0.177
$Room_{rtu}$	0.03	0.03	0.04	0.02	0.05	0.04	0.033
$Power_{rtu}$	0.11	0.05	0.15	0.06	0.07	0.05	0.088
$\Delta T_{zone_}sp$	0.32	0.44	0.30	0.38	0.44	0.49	0.376
RTU_{stage}	0.27	0.29	0.26	0.32	0.22	0.25	0.272

5.2.3 Calculation of Alternative Matrix

When the alternative matrix is calculated to curtail RTUs, the load-shedding candidates can be determined based on the ON status of the RTUs. Table 6 shows the example of an RTU input data set of criteria to make the alternative matrix. The input data include the two temperature measurements ($T_{zone\ at\ t-\delta}$ and $T_{zone\ at\ t}$), T_{sp} , n_{rtu} , $Room_{rtu}$, $Power_{rtu}$, and RTU_{stage} corresponding to each RTU.

Table 6. Example of RTU input data for the alternative decision matrix

Criterion	Unit	RTU-1	RTU-2	RTU-3	RTU-4	RTU-5	RTU-6	RTU-7
n_{rtu}	[ea]	1	1	1	1	1	1	2
$T_{zone\ at\ t-\delta}$	°F	76.17	74.85	72.71	75.59	74.53	75.01	76.17
$T_{zone\ at\ t}$	°F	76.21	73.51	71.21	74.88	71.51	74.07	76.21
$Room_{rtu}$	[-]	Office	Director's Office	Kitchen	Office	Computer Lab	Conference Room	Office
$Power_{rtu}$	[kW]	7.2	1.8	3.2	6.9	3.5	2	7.4
T_{sp}	[°F]	75	72	71	72	71	73	73
RTU_{stage}	[ea]	1	1	1	1	1	1	1

Table 7 shows the example of matrix B_{normal} , which includes the weight of each criterion associated with each alternative load (RTUs) according to the pair-wise comparisons and the input data. The comparison reflects the intensity as indicated by the ratios of the numerical values that preserve the strength of alternative preferences.

Table 7. Example of the alternative decision matrix of RTUs

Criterion	RTU-1	RTU-2	RTU-3	RTU-4	RTU-5	RTU-6	RTU-7
n_{rtu}	0.11	0.11	0.00	0.22	0.22	0.22	0.11
ΔT_{zone_d}	0.00	0.18	0.20	0.09	0.40	0.13	0.00
$Room_{rtu}$	0.16	0.05	0.16	0.16	0.05	0.26	0.16
$Power_{rtu}$	0.23	0.06	0.10	0.22	0.11	0.06	0.23
ΔT_{zone_sp}	0.27	0.21	0.00	0.11	0.00	0.30	0.10
RTU_{stage}	0.14	0.14	0.14	0.14	0.14	0.14	0.14

5.2.4 Calculation of Decision Priority Vector

The example of decision priority vector C of alternatives can be calculated by multiplying eigenvector, A_p , and matrix, B_{normal} , thus determining dynamic prioritization of the loads. As can be seen in Table 8, the ILC process prioritizes the RTUs for curtailment (priority of 1 implies that it will be curtailed first). Once the loads are prioritized for curtailment, the number of RTUs that need to be curtailed to meet the peak demand can be determined based on their current power consumption.

Table 8. Example of the decision priority vector for load curtailment

	RTU-1	RTU-2	RTU-3	RTU-4	RTU-5	RTU-6	RTU-7
Priority Weight	0.17	0.16	0.09	0.13	0.13	0.20	0.11
Priority	2	3	7	5	4	1	6

5.2.5 Load Control Based on the Decision Priority Vectors

Table 9 shows the example of the current power consumption of each of the seven RTUs and the current demand estimate for this example data set is 36 kW, as previously mentioned in Section 5.1. Estimation of the expected power contribution of each RTU is obtained from a $Power_{rtu}$ describing the rated input power consumption because the usage of the individual RTUs is not measured directly on permanent basis. With the RTU switch on, it is assumed that the thermal load is exactly matched by the rated power consumption of the RTU. Based on a target demand of 30 kW as described earlier in Section 5.1, curtailing RTU-6 and RTU-1 (based on the decision priority shown in Table 8) will bring the total consumption below 30 kW.

The temperature offset was used to raise the current set point of selected RTUs during the period of curtailment. The temperature offset raises the thermostat set point by a fixed amount. For example, the curtailment can be implemented by raising the zone set point from 72°F to 76°F, as shown in Table 9. As the set points are raised, the compressors of the RTUs will be turned off until 1) the zone temperature exceeds the set point and 2) the curtailment time period of ILC ends.

When initiating RTU shutdown, the curtailment time period for which the RTUs can be kept in the OFF state, starting from the current state, is determined. When an RTU is curtailed for a part of the curtailment time, it is allowed to come on again when it reaches its maximum allowed temperature. If the estimated demand is exceeded during the curtailment time period, the ILC algorithm will identify additional RTUs based on priority vector, and the curtailment time period for all curtailed RTUs will be extended. When ending the curtailment time period, the ILC algorithm will identify the RTUs that have been curtailed and that could be switched on by decreasing the zone set point from 76°F to 72°F.

Table 9. Example of RTU set points based on the decision priority vector

	RTU-1	RTU-2	RTU-3	RTU-4	RTU-5	RTU-6	RTU-7
RTU Power kW	6.8	2.8	5.4	6.8	5.4	2.8	6.8
Tsp °F	76	72	72	72	72	76	72

6.0 Simulation Results and Discussion

A small commercial building simulation model was used to evaluate and validate the ILC process. Kim et al. (2015) developed a three-zone building for simulating the dynamic indoor environments and building envelopes using a reduced-order coupled computational fluid dynamics model. The simulation model was validated by using measurements from the field site. For detailed the description and validation of the simulation model, please refer to Kim et al. (2012 and 2015). Table 10 shows the summary of building simulation conditions. A 1-month simulation was performed to study the potential for reducing the peak demand using ILC. The peak demand is assumed to be the highest average power consumption measured in a rolling 15-minute period. The weather data from 2014 TMY3 (Typical Meteorological Year) was used for the simulations.

Table 10. Major building simulation parameters.

Input	Condition
Simulation time periods	One month from July 15 to August 14
Outdoor air temperature data	TMY3
Building type/location	A restaurant/Philadelphia
Building size	70 ft. width/65 ft. depth/11 ft. height
Building occupancy time	9:30 a.m. to 10:00 p.m.
Normal occupied/unoccupied set points	71.5/75.0 [°F]
AHP occupied set point	80.0 [°F]
Thermostat temperature dead band	± 0.5°F
RTU compressor minimum run time	5 minute
Thermostat delay time	5 minute

Four RTUs serve the open-spaced (without walled-in spaces) building. The room/zone priority is the same for all RTUs because they serve an open space. RTU-1 and RTU-3 serve the dining area and RTU-2 and RTU-4 serve the wine bar. The supply air fans of all RTUs are ON continuously when the building is occupied. RTU-1 has two refrigerant circuits with a nominal cooling capacity of 15 tons. Each of the two compressors is connected to a separate condenser. The other three RTUs have a 4-ton cooling capacity with one refrigerant circuit each. The coefficient of performance of RTU-1 is approximately 35% higher than the others. All RTUs are controlled by a thermostat with a fixed occupied set point of 71.5°F and a dead band of ± 0.5°F. The second compressor of RTU-1 turns ON when the space temperature is 1.0°F above its cooling set point. To avoid short cycling of the RTU compressors, the RTU is run for some minimum period before it is turned OFF. After a change in thermostat set point, the thermostat typically responds with a time delay. The RTU compressor minimum run time and thermostat delay time are set at 5-minutes each. After the set points are changed, there is a delay—the thermostat delay time—before the thermostat applies the change.

The zone temperature set point is increased to turn OFF the corresponding RTU that is chosen by the assigned priority order. When the load curtailment ends, the set points are returned to their original values. For RTUs that have a single compressor, the set point during curtailment is 75.6°F. The multi-stage RTUs are considered multiple single-stage RTUs. The RTU-1 is considered to be two separate single-stage RTUs. To turn OFF the second compressor of RTU-1, the set point is set to the current zone temperature served by RTU-1. When an RTU is OFF during prioritization, it is excluded from the priority

decision. If an RTU is turned OFF by the ILC process and the zone temperature corresponding to that RTU exceeds the new set point, then the RTU is allowed to resume its operation.

6.1 Case Study: Analysis and Validation of Intelligent Load Curtailment with Different Curtailment Time Periods

This section discusses the curtailment time period related to its influence on the results of the process. Figure 5 shows how the time period affects peak demand management. The targeted peak demand is set to 30 kW and it roughly corresponds to 85% of the base case peak demand. The time period refers to the minimum time the unit remains OFF to meet the target. Three different time periods—5, 15, and 30-minutes—were considered to evaluate the effect of the time period on peak demand management. When the electric power is higher than 30 kW, the RTUs are curtailed using the priority order to reduce the demand by 6 kW because the base peak is 36 kW. The ILC process increases the zone set point of the RTUs selected for curtailment, which results in those units turning OFF. The normal zone set points are restored after the time period ends. For example, if the ILC time period is 15-minutes, the curtailed RTU will remain OFF for 15-minutes. However, during this 15-minute period, if the zone set point exceeds the new zone set point, the unit will be released from curtailment and allowed to run. The short time periods (upper right graph in Figure 5 **Error! Reference source not found.**) can lead to more frequent cycling of the RTUs but can result in less discomfort to the occupants. The long time period (lower right graph in Figure 5) prevents short cycling but may result in more occupant discomfort.

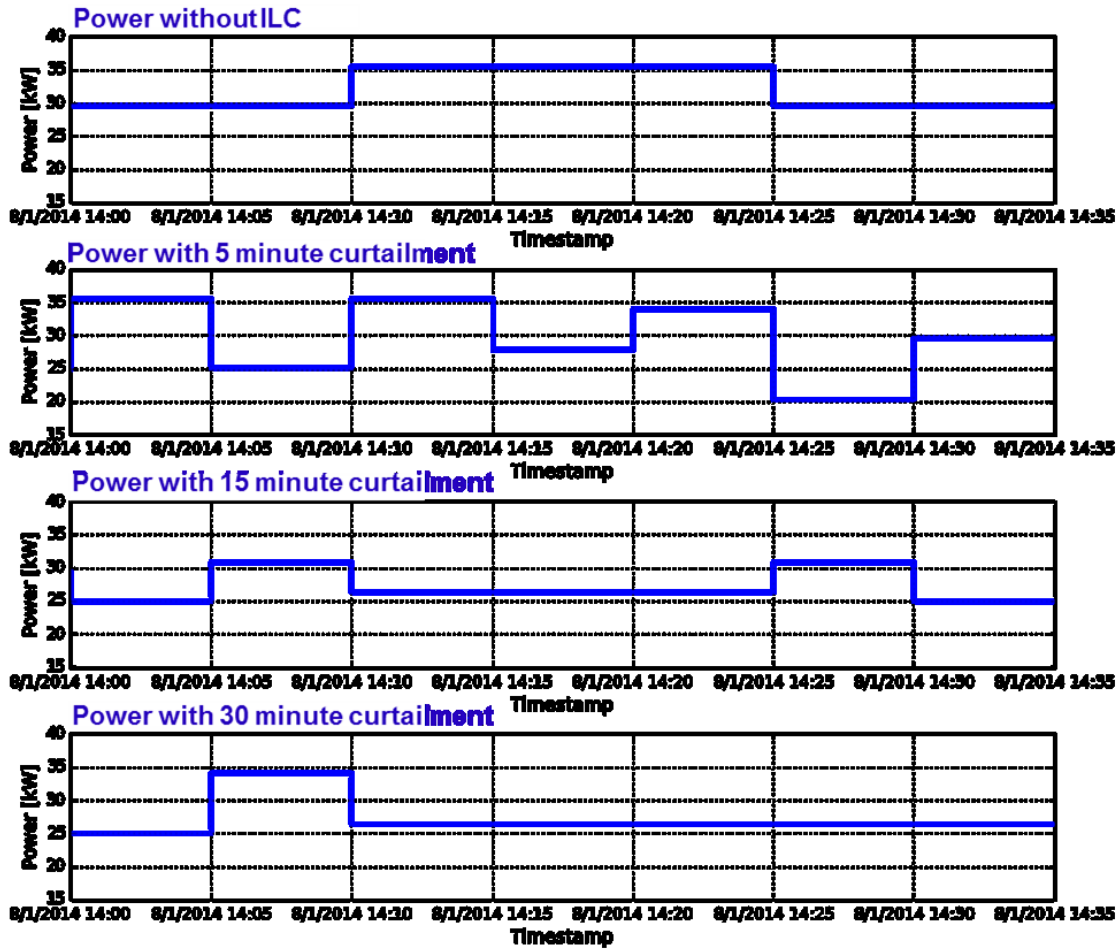


Figure 5. Electricity consumption profile under different ILC time periods

Weekly electricity consumption profiles for different time periods are shown in Figure 6. The week between July 25 and August 2 was chosen because it was one of the hottest weeks of the year. The blue line (in Figure 6) represents the electric consumption profile, the top of the yellow shaded area represents the peak consumption with conventional operations, and the bottom of yellow shaded area indicates the new demand target with ILC in operation. With conventional control, the peak demand is approximately 36 kW. The goal of the ILC process is to maintain the peak under 30 kW. With the ILC time period of 5-minutes, the peak demand at times is higher than 30 kW. When ILC is operated using 15- and 20-minute time periods, the process is able to achieve the goal at all times. The peak demand is much smoother, with fewer fluctuations, for higher time periods. The ILC operation using 15- and 30-minute time periods can also prevent the “rebound” that occurs during equipment recovery, compared to ILC using 5-minute time periods.

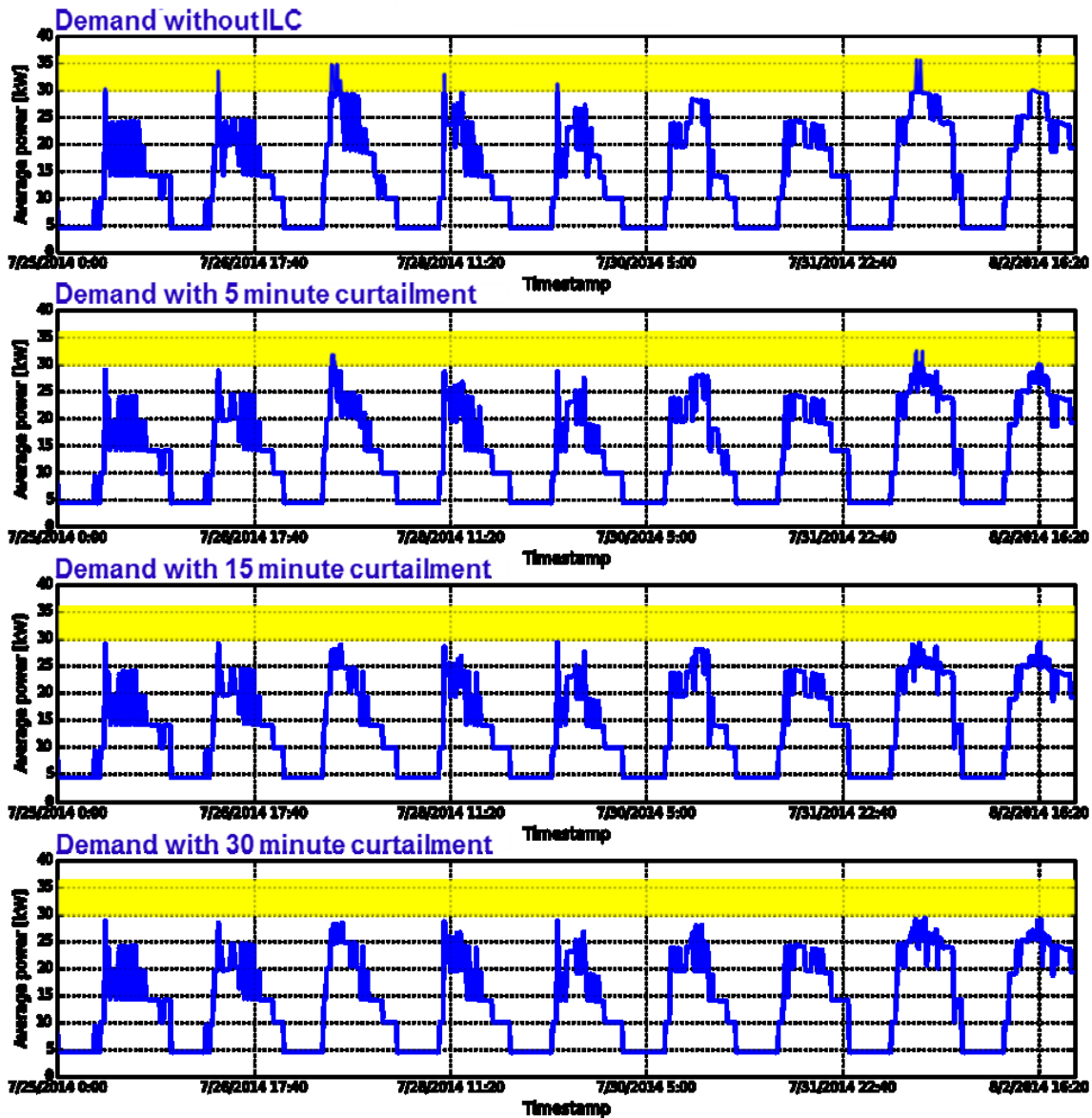


Figure 6. Weekly electricity consumption profiles under different ILC time periods

Because the zone set points are raised during ILC operation, the zone temperatures will be typically higher than normal in the cooling mode and lower than normal in the heating mode. Figure 7 shows how ILC affects the zone temperature with the varying ILC time periods. The edges of the yellow shaded area represent the upper and lower bounds of comfort in the cooling mode. The occupied and unoccupied cooling set points are 71.6°F (horizontal red line) and 75.6°F, respectively. The black line represents the unoccupied zone temperature, whereas the occupied zone temperature is marked with a solid color line. When the building is unoccupied, the temperature set point is increased to a higher value leading to an increase in the zone temperature. To manage the peak demand target, the ILC process raises the set point of the RTUs based on the priority list. Although the temperature difference between the conventional (uncontrolled) and ILC approaches increases with the time periods, the zone temperatures for all four RTUs remained below the upper comfort temperature boundary during the occupied period. For example, the deviation of zone temperatures from the normal set point with the ILC time period of 30 minutes is

between 2°F and 3°F higher. The space temperatures show values that drop to as low as 65°F during the nighttime. The simulation model was developed based on linearization on the hot summer days. Therefore, the model could have unrealistic behavior if the system operates too far away from the linearized conditions (Kim et al. 2015). Overall, the ILC algorithm using 15- and 30-minute time periods can reduce the peak loads by controlling the RTUs, while still maintaining reasonable thermal comfort.

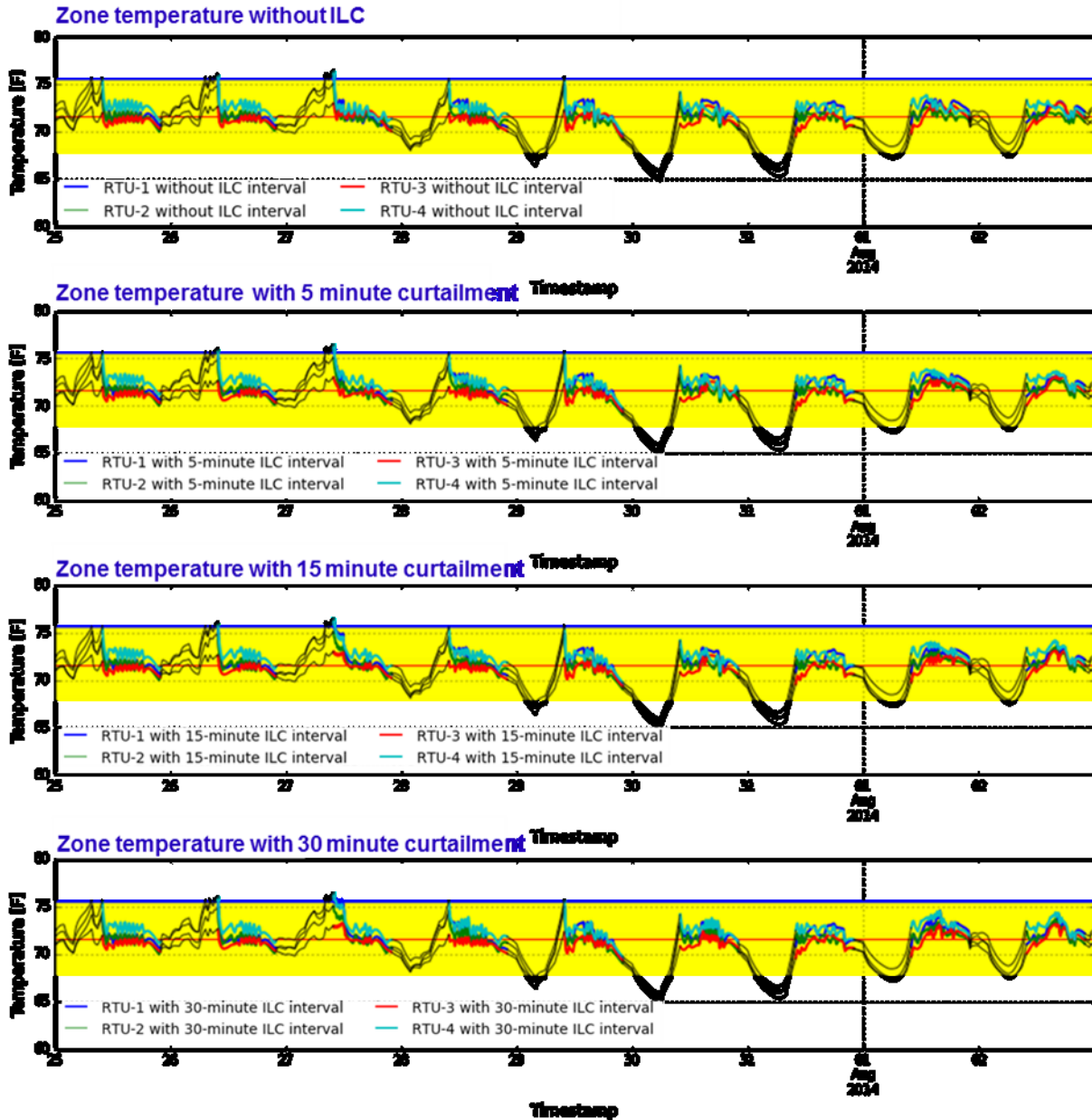


Figure 7. Zone temperature profiles for different ILC time periods

Table 11 shows the maximum and average temperature for each RTU during the occupied time period during a 1-month operating period. As seen from the data, the ILC process did not result in a significant

zone temperature rise when the units were curtailed to achieve the peak demand goal. For example, the ILC process using a time period of 30-minutes showed an average and maximum temperature rise of 0.4°F and 1.9°F, respectively, compared to the conventional control during the occupied period. Overall, the ILC process using 15- and 30-minute time periods can maintain occupant comfort while successfully limiting peak demand.

Table 11. Comparison of zone temperatures under different ILC time periods

	Maximum Zone Temperature (°F)				Average Zone Temperature (°F)			
	Normal	ILC Time Period (minutes)			Normal	ILC Time Period (minutes)		
		5	15	30		5	15	30
RTU-1	73.5	73.6	74.7	75.5	72.6	72.6	72.6	72.8
RTU-2	72.6	72.9	73.4	74.8	71.8	72.1	72.1	72.3
RTU-3	73.1	73.1	73.1	74.3	71.8	71.9	71.9	71.9
RTU-4	73.8	74.0	74.5	75.9	72.7	73.0	73.3	73.4
Average	73.3	73.4	73.9	75.2	72.2	72.4	72.4	72.6

Table 12 shows the RTU ON-OFF cycles and compressor runtimes during a one-month operating period. The results show that RTU-1 with stage 2, RTU-2, and RTU-3 cycled more often to meet the targeted peak demand under the ILC than under normal control. The number of ON-OFF cycles of RTU-1 with stage 1 and RTU-4 were almost constant regardless of the ILC time period. As the ILC time period decreases, there is an increase in the on/off cycling and a decrease in the runtime of the RTUs. For example, the ILC using the 5-minute time period results in 4% fewer run hours and 27% more ON-OFF cycling compared to normal control. As the ILC time period increased, the ON-OFF cycling rates were significantly reduced. For instance, ILC using the 30-minute time period results in almost 6% fewer run hours and 12% more ON-OFF cycling compared to normal control. The RTU-1 has two refrigerant circuits, which allow modulation of the compressor staging and result in less ON-OFF cycling. The result indicates that the ILC process can provide modest energy savings while managing the peak with a small impact on the thermal comfort. Therefore, the ILC process can provide cost savings derived from both reductions in energy use and peak charges. Overall, the ILC process using the 15- and 30-minute time periods should be considered.

Table 12. RTU ON-OFF cycles and run times under different ILC time periods

Time Period	The Number of ON-OFF Cycles				Run Time (hours)			
	Normal	ILC Time Period (minutes)			Normal	ILC Time Period (minutes)		
		5	15	30		5	15	30
RTU-1-1	387	381	383	381	243.8	248.5	249.4	250.2
RTU-1-2	78	106	114	120	8.7	10.3	11.9	11.3
RTU-2	272	416	324	316	127.5	118.2	118.2	119.4
RTU-3	36	76	88	72	64.2	40.3	32.6	18.0
RTU-4	109	141	125	101	381.4	378.8	378.7	380.7
Total	882	1120	1034	990	826	796	791	780
Comparisons	Baseline	27% ↑	17% ↑	12% ↑	Baseline	4% ↓	4% ↓	6% ↓

6.1.1 Case Study: Analysis and Validation of Intelligent Load Curtailment with Different Target Peak Demand Values

This section discusses the simulation results that demonstrate how the target peak demand control affects RTU ON/OFF control and thermal comfort. The ILC algorithm has the capability to adjust the target peak demand that needs to be shed. To efficiently operate the ILC algorithm, the target level for peaks in demand should be optimally chosen. For example, if the building operator adjusts the target peak demand to a value that is too high, occupant comfort may be affected because significant RTUs will be automatically adjusted to reduced operations. Furthermore, secondary peaks in demand may be caused if the initial target level for peak demand is not optimally chosen. To analyze the impact of target peak level in ILC, three different target peak demand values of 30, 27, and 25 kW were considered. The runtime interval was set to 15-minutes. The proposed control strategy was implemented to find an optimal trade-off between conflicting objectives of demand savings and comfort level in a simulation test bed. The impact of different target peak demand values were evaluated using simulation results.

Figure 8 shows the continuous weekly profiles of electrical demand for different target peak demand values. ILC achieved 19, 28, and 33% demand reduction ratios compared to conventional control. For all cases, ILC was able to manage the peak load reduction below target demand. For the target of 27 kW, ILC maintains the zone temperature within the comfort range but it switches more frequently than conventional control. For the target peak demand value of 25 kW, significant cycling occurred at the occupied time that peak demand occurred. Significant cycling occurred because of small cooling capacities for the time being compared to the cooling loads in the building.

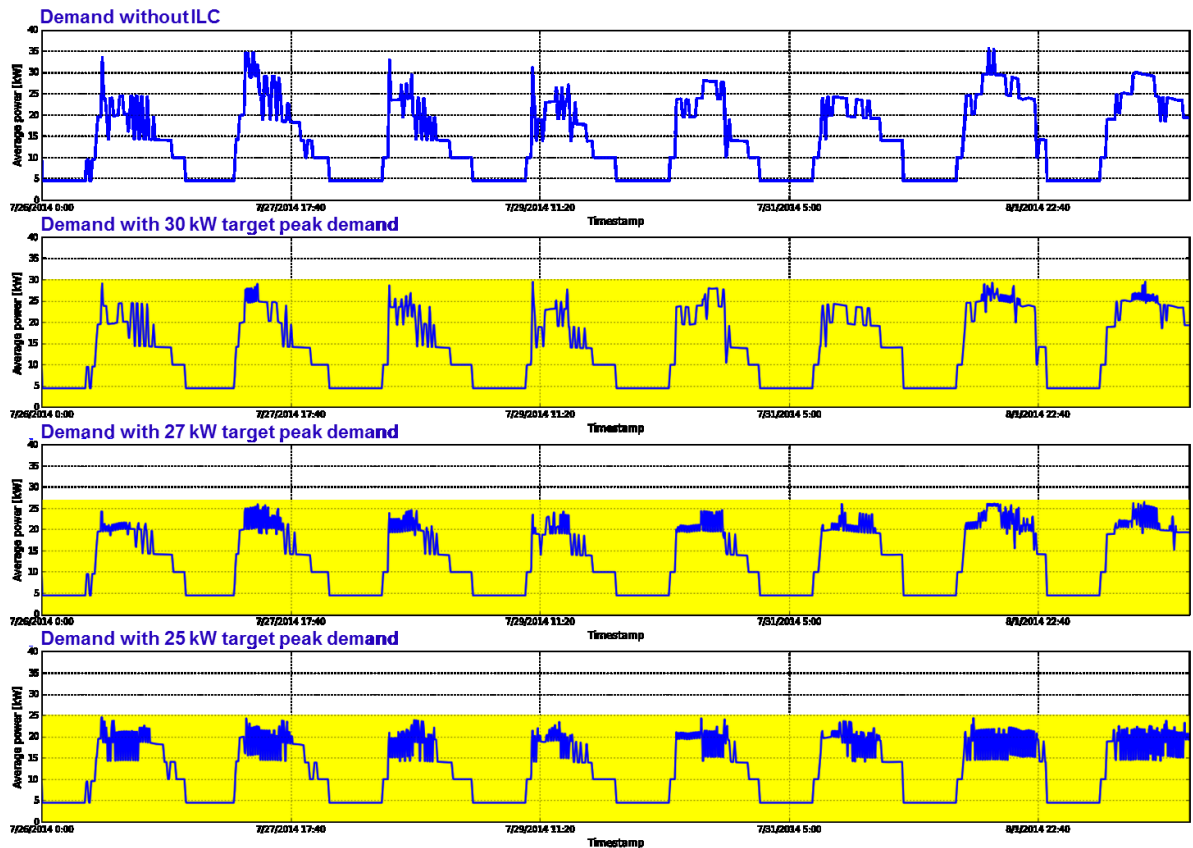


Figure 8. Electric demands under different target peak demand values

Figure 9 shows the weekly zone temperature profiles under conventional and ILC operation with different target peak demand values. As the target peak demand value is reduced, significant gaps occur between the set point and zone temperatures and the spatial variation of temperatures between the zones. For target peak demand values of 27 and 30 kW, the zone temperature was maintained within the comfort limit during the occupied period. The ILC with a target of 25 kW showed a significant occupied temperature rise for the curtailed RTU during the occupied time period. Temperatures for target 25 kW are around 5 °F to 6 °F higher than temperatures for target 30 kW during the occupied time. Compared to conventional control, the zone temperatures for RTU-1, RTU-2, and RTU-4 increased more quickly and approached 80 °F for a short period of time under ILC. ILC to keep the peak demand below 25 kW would turn OFF a relatively large number of RTUs. Overall, the comfort problems occurred because the target level for peak demand was not optimally chosen.

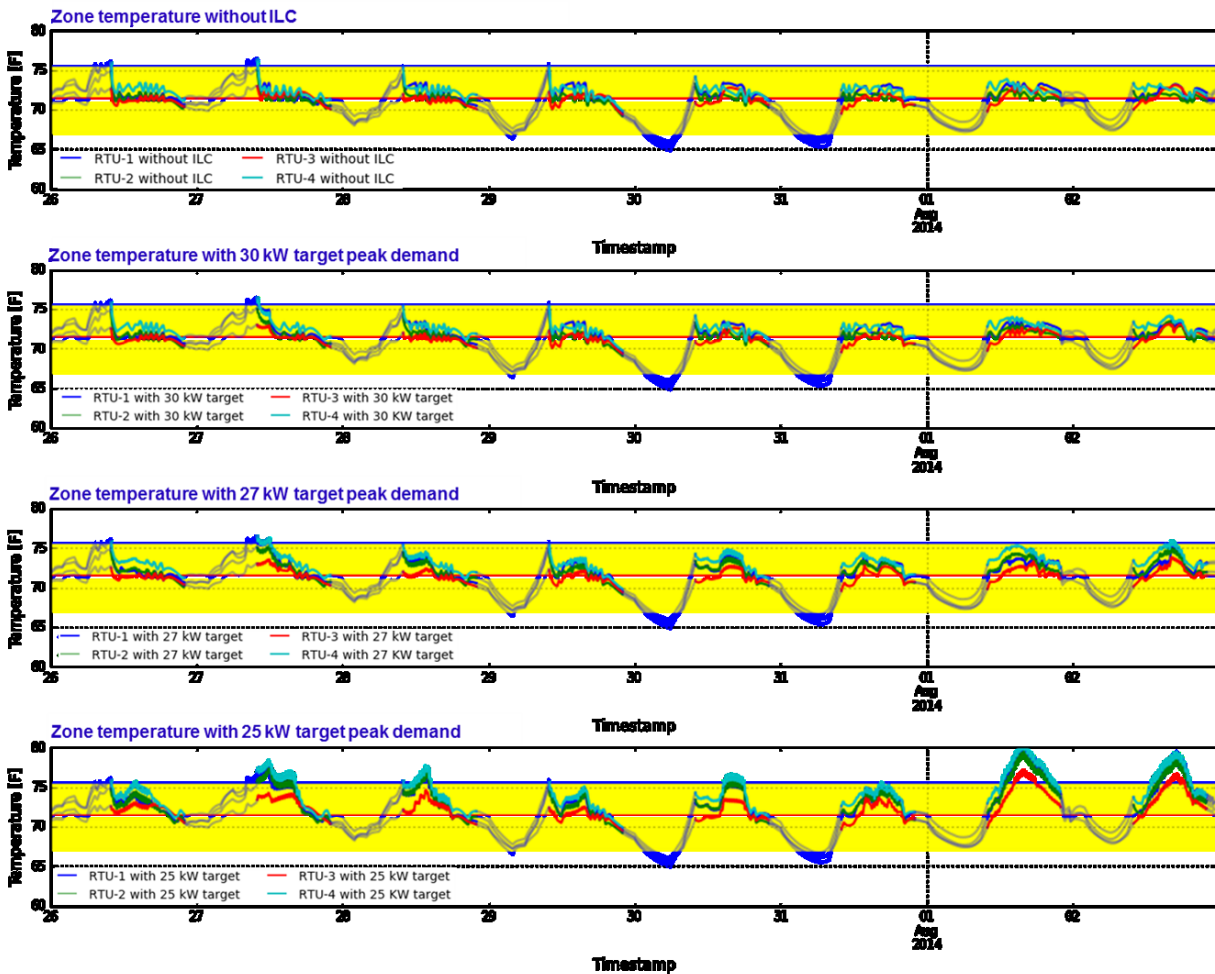


Figure 9. Zone temperature profile under different target peak demand values

Table 13 shows the maximum and average temperature for each RTU during the occupancy time period for 1 month. The ILC with target peak demand values of 27 and 25 kW showed a maximum temperature rise of 3.7°F and 6.3°F, respectively, compared to the conventional control during the occupied time period. For the target of 25 kW, because of low utilization of RTUs for ILC, zone temperatures exceed the comfort temperature bounds. The zone temperature could not be maintained without using a large-capacity RTU-1. Although the maximum zone temperature was approaching 80°F at the end of the peak

period, the average occupied zone temperature was 75°F during these hot days. As a result, it was demonstrated how the prediction of future demand can be used to maintain the target peak at an optimal level without harming the comfort of building occupants.

Table 13. Comparison of zone temperatures under different target peak demand

Time Period	Maximum Zone Temperature (°F)				Average Zone Temperature (°F)			
	No Demand	Demand 30 kW	Demand 27 kW	Demand 25 kW	No Demand	Demand 30 kW	Demand 27 kW	Demand 25 kW
RTU-1	73.5	74.7	77.8	80.4	72.6	72.6	73.0	76.4
RTU-2	72.6	73.4	77.0	79.9	71.8	72.1	73.0	75.9
RTU-3	73.1	73.1	75.2	77.1	71.8	71.9	71.9	74.2
RTU-4	73.8	74.5	78.0	80.9	72.7	73.0	74.0	74.4
Average	73.3	73.9	77.0	79.6	72.2	72.4	73.0	75.2

Table 14 shows the RTU ON-OFF cycles and compressor runtime (hours) under different target peak demand values. As the target peak demand value decreases, then the number of ON/OFF cycling increases and the runtime of the RTUs decrease. For the number of ON/OFF cycles, ILC with a target peak demand value of 25 kW is three times higher than the conventional control. The reduction in the RTUs runtime due to ILC with a target peak demand value of 27 kW is 11% of the conventional control. Therefore, the ILC can provide an annual energy cost savings in both electrical consumption and peak demand charges.

Table 14. RTU ON-OFF cycles and runtime under different target peak demand values

Time Period	Number of On-Off Cycles during One Month				Runtime (hours) during One Month			
	No Demand	Demand 30 kW	Demand 27 kW	Demand 25 kW	No Demand	Demand 30 kW	Demand 27 kW	Demand 25 kW
RTU-1-1	387	383	417	577	243.8	249.4	244.8	212.1
RTU-1-2	78	114	302	480	8.7	11.9	15.3	20.6
RTU-2	272	324	526	656	127.5	118.2	82.3	87.0
RTU-3	36	88	234	422	64.2	32.6	29.4	26.4
RTU-4	109	125	249	405	381.4	378.7	359.5	327.4
Total	882	1034	1728	2540	4128	3954	3657	3368
Comparisons	Baseline	17% ↑	96% ↑	188% ↑	Baseline	4% ↓	11% ↓	18% ↓

7.0 Discussion of Field Test Results

The ILC algorithm (also known as v-agent when deployed on VOLTTRON platform) using the VOLTTRON platform was demonstrated at a PNNL mechanical shop building that included office space in Richland, Washington. The objective of the experimental demonstration was to minimize the peak demand over a demand period of 30-minutes during the specific month. The system characteristics are summarized in Section 7.1 and comparisons between operating 1) with ILC and 2) without ILC are provided in Section 7.2. Although the ILC agent based on the VOLTTRON platform was implemented for 7 months, only selected data are presented in the comparisons.

Figure 10 shows the external view of the building located on PNNL campus. Ten heat pumps are located on the roof of the building, as shown in Figure 11. The 10 heat pump systems serve three different areas in the building. Heat pumps 1a, 1b, 2, 7, and 14 serve the office area, heat pumps 4, 5, 6, and 8 serve the shop, and heat pump 3 serves kitchen area. As shown in Figure 11, the heat pumps with smaller capacities serve the office area, while those with larger capacities serve the shop.

Implemented earlier this year, ILC began controlling the operation of multiple heat pumps serving offices and other work spaces. The deployment site used the building automation system and had access to key variables and control such as zone temperature, set point, and the compressor states of the heat pumps. Some integration development and testing was performed to obtain the desired communications functionality between VOLTTRON running the ILC agent (coded in Python) and the building automation system. After that, additional functional testing of the ILC algorithm was performed to verify safe operation. For example, initially some heat pumps failed to change the heating temperature set point but this was because the set point was set for read-only mode. After initial testing, the setting was changed to write/read mode.



Figure 10. External view of the building on PNNL campus

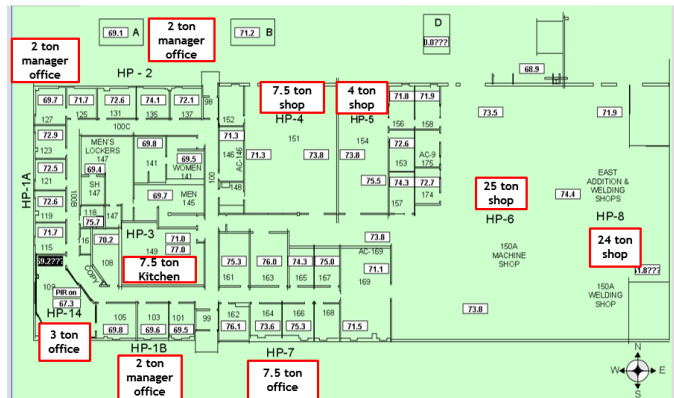


Figure 11. Location of heat pump in the building on the PNNL campus

The specifications of the heat pumps in the building are given in Table 15. Three heat pumps, named 1A, 1B, and 2, have one refrigerant circuit that has a nominal cooling capacity of 3 tons each and an electric heater capacity of 7.5 kW. Three heat pumps named HP-3, HP-4, and HP-7, have two compressors that have a nominal cooling capacity of 7.5 tons each and an electric heater capacity of 14 kW. Two heat pumps, named HP-6 and HP-8, have a nominal capacity of 25 tons each with an electric heater capacity of 72 kW and 20 tons each with an electric heater capacity of 54 kW using two circuits with two compressors and two condenser fans. Two heat pumps, named HP-5 and HP-14 have a nominal capacity

of 4 tons each with an electric heater capacity of 13 kW and 3 tons each without an electric heater. For testing, we controlled the compressor and electronic heater of the heat pumps separately, as if they are two different systems. For example, we could leave the compressor ON, while the electric heater was turned OFF. This approach would have given us 19 testing systems. ILC would then control the 19 systems to manage peak demand while still maintaining reasonable thermal comfort.

Table 15. Details of the heat pumps

	Heat Pump Unit	Capacity [tons]	Electric Heater Capacity [kW]	Compressor [ea]	Room Type
1	HP-1A	2	7.5	1	Manager Office
2	HP-1B	2	7.5	1	Office
3	HP-2	2	7.5	1	Manager Office
4	HP-3	7.5	14	2	Lobby
5	HP-4	7.5	14	2	Shop
6	HP-5	4	13	1	Shop
7	HP-6	25	72	2	Shop & Office
8	HP-7	7.5	14	2	Office
9	HP-8	20	54	2	Shop
10	HP-14	3	-	1	Office

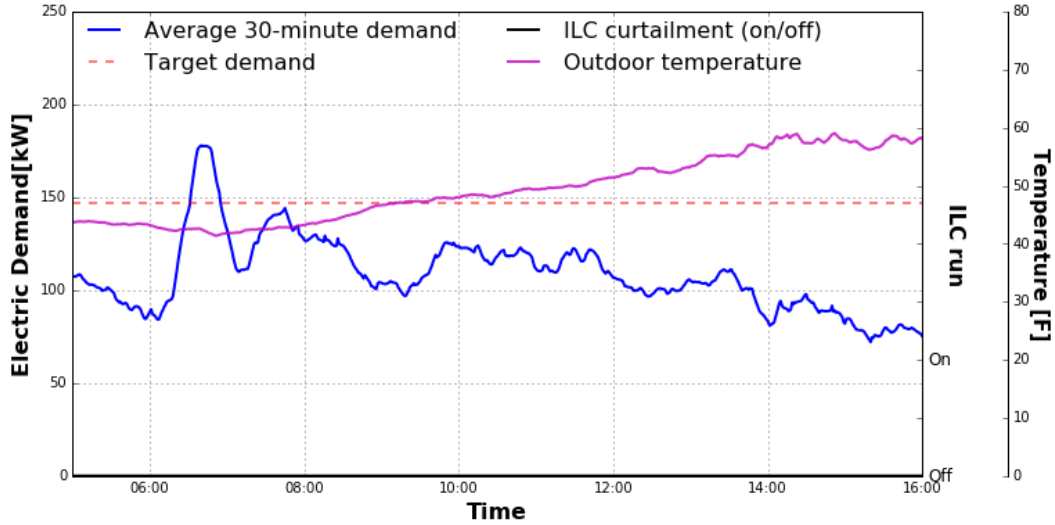
7.1 Field Test Results for ILC

Field test results indicated that ILC managed the peak demand within an acceptable target peak level based on WBE prediction, as well as zone temperatures reflecting the comfort status of building occupants. Because weather and internal gains keep changing, the performance validation of the ILC algorithm is difficult in practice. To compare the results with and without ILC running, the ILC algorithm was run one day and normal operations the following day.

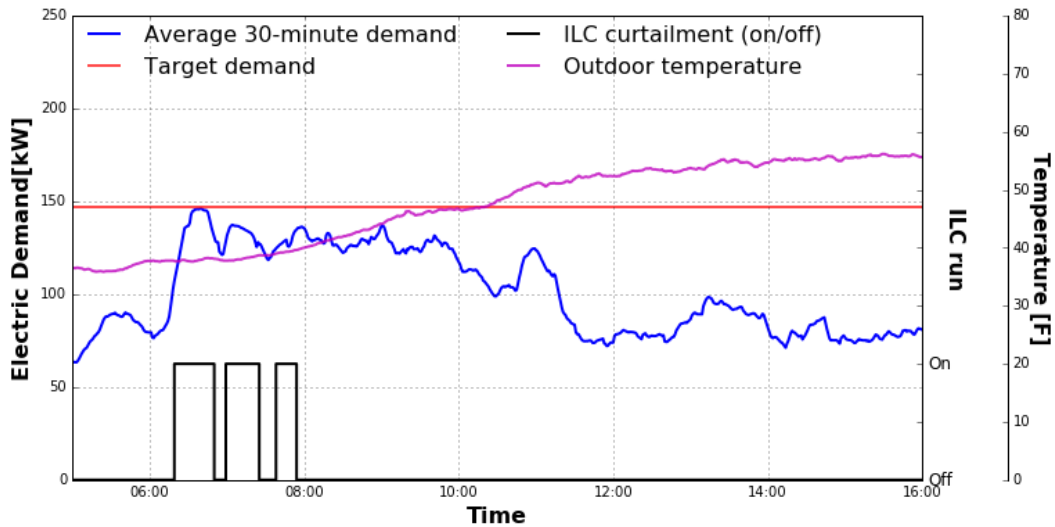
7.1.1 Field Test Results for ILC during the Heating Season

Figure 12 shows the sample results under (a) no ILC (March 14) and (b) with ILC (March 15). The blue, red, purple, and black lines indicate an average 30-minute rolling window of target demand, outdoor temperature, and ILC run signal, respectively. The target demand is determined at 145 kW. For the peak demand, the measured power data were summed and a moving average method with a 30-minute time interval was used in calculating the electric demand. The maximum peak demand, 180 kW, occurred during the morning warm-up period, between 6 a.m. and 8 a.m., as shown in Figure 12a.

Figure 12b shows the ILC test results from March 15. When building energy consumption peaked in the morning, ILC quickly prioritized heat pump operations, shutting down some units while running others. There were three possible periods when the building 30-minute average peak could have exceeded the target peak demand level. The ILC algorithm controlled the heat pump systems to avoid exceeding the peak demand level. Overall, the results show that the ILC algorithm was able to control the system and keep it under the demand level of 145 kW. Results show the ILC algorithm achieved about a 20% peak demand reduction compared to the results under no ILC operations.



(a) Sample result under no ILC (March 14)



(b) Sample result under ILC (March 15)

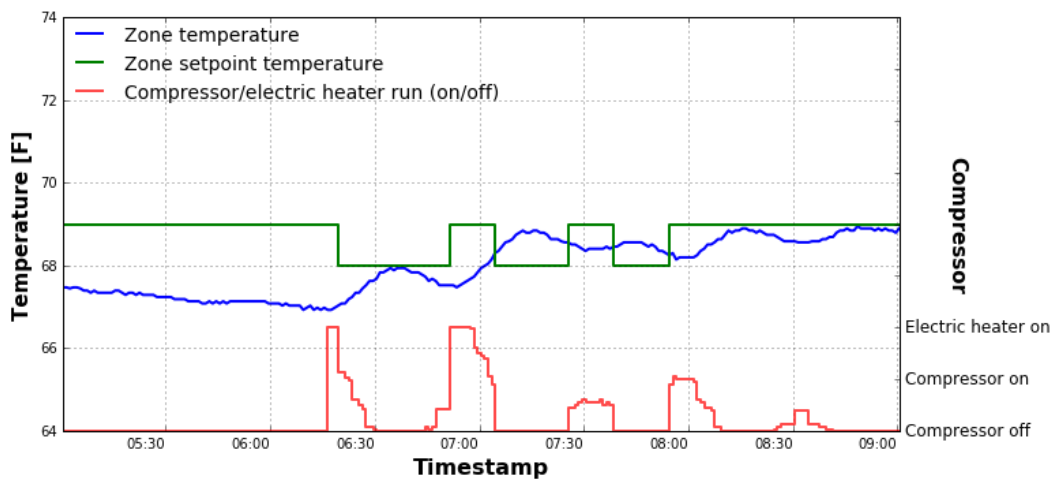
Figure 12. Electric demand and outdoor temperature profiles during the heating season

Figure 13 shows example temperature and heat pump status signal profiles derived under ILC on March 15. The blue line represents the zone temperature, the green line is the set point of heat pump system, and the red line is the operation status of the heat pump. Both heat pumps have a compressor unit with electric heaters. Output stages of heat pump systems is shown on the second y-axis indicate the compressor and electric heater of heat pumps, respectively. The OFF state is denoted as 0 in the figures.

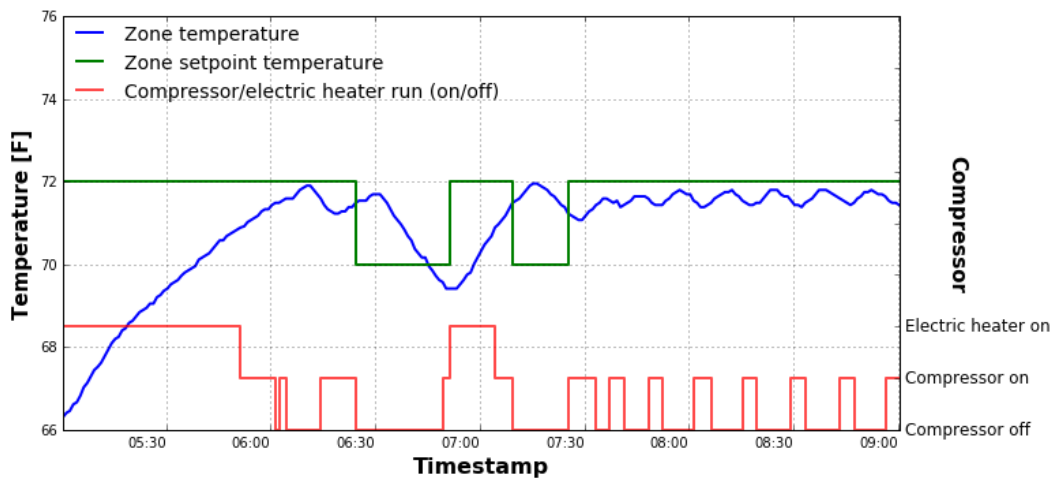
When the zone temperature was decreased more than 2°F below the set point, both the heaters and compressor would be turned ON at the same time. To prevent this, the offset value of each heat pump was determined to be less than 2°F in accordance with building operator’s opinion. For example, the set point offset was set to 1°F for heat pump 8 and 2°F for HP-4—lower than the normal set point. When the ILC event ended, the set points returned to their original values.

The zone temperature of HP-8 decreased less than 1°F compared to the temperature before the compressor and electric heater were turn OFF during all ILC events. During the first ILC event, HP-8 continued its heating operation when the zone temperature was less than the set point. The compressors were subsequently turned OFF after all electric heaters were turned OFF. After the second and third ILC events, only the compressor turned ON because the zone temperature decrease was less than 1°F below the set point. When all ILC events ended, the compressors of heat pumps were operating more of the time to meet the heating load.

During the ILC event, the set point of HP-4 was lowered by 2°F from the original set point. ILC did not result in a significant zone temperature decrease when the HP-4 was curtailed to manage the peak demand level. For example, the maximum deviation in zone temperatures from the normal set point after the first ILC event was between 2°F and 3°F. Overall, ILC successfully dropped demand in some spaces to meet the established limit, and occupants did not indicate any comfort impacts.



(a) HP-8



(b) HP-4

Figure 13. Example of temperature and heat pump status signal profiles during ILC (March 15)

Table 16 shows the summary of curtailment of each heat pump during ILC on March 15. In the table, the symbol “O” indicates that ILC lowered the set point of the heat pumps selected for curtailment, which

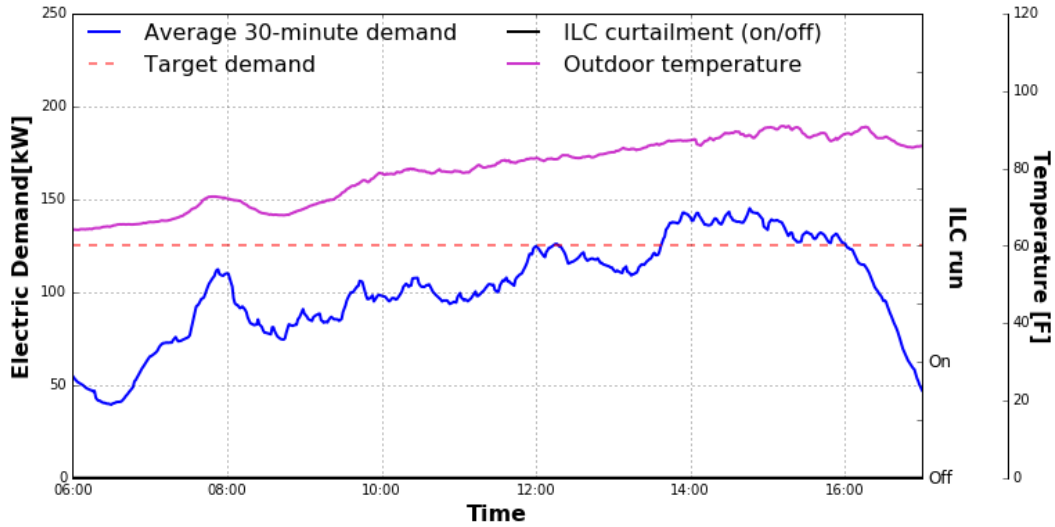
results in those units turning OFF. The ILC uses HP-8 as much as possible and minimizes the use of the other heat pumps to reduce the demand, because the electric heater power of HP-8 is far greater than the other heat pumps.

Table 16. Summary of curtailment of each heat pump during ILC (March 15)

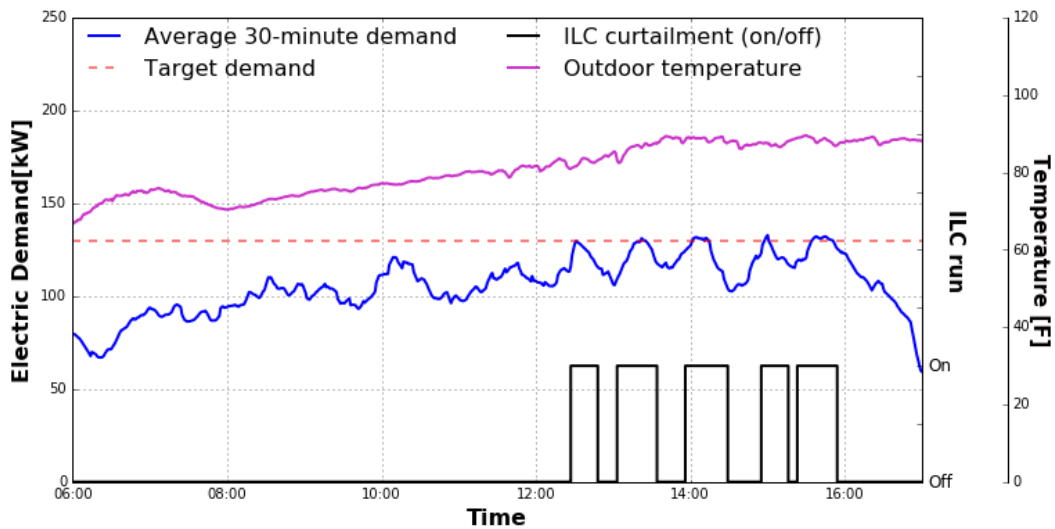
System Model	Room Type	Capacity [tons]	Electric Heater kW	1 st ILC	2 nd ILC	3 rd ILC	Number of Curtailments
HP-1A	Manager Office	2	7.5		O		1
HP-1B	Office	2	7.5	O			1
HP-2	Manager Office	2	7.5				0
HP-3	Kitchen	7.5	14				0
HP-4	Shop	7.5	14	O	O		2
HP-5	Shop	4	13	O			1
HP-6	Shop	25	72				0
HP-7	Office	7.5	14	O			1
HP-8	Shop	20	54	O	O	O	3
HP-350	Office	3	7.5				0
Total Heat Pump Curtailments				5	3	1	9

7.1.2 Field Test Results for ILC during the Cooling Season (July)

Figure 14 shows the test results obtained in July under (a) no ILC and (b) with ILC. As the outdoor temperature started to rise in July, the maximum outdoor temperature was measured at about 90°F. As mentioned, the building controls were alternated daily to validate the ILC algorithm. For example, ILC was run on July 11 but not on July 12. Figure 14a shows the maximum peak demand as 148 kW between 2 and 4 p.m. when the outdoor temperature reached maximum. Figure 14b shows the demand profile under ILC. The target was set at 125 kW as determined using the WBE method. There were five peak demand events between noon and 4 p.m. As shown, each time the building peak was closed to the target, ILC curtailed some RTUs to manage the peak under the demand level of 125 kW. The duration of each ILC event varied because secondary peak demands occurred during some events. In these cases, other heat pumps were turned ON because the zone temperatures were higher than the set points.



(a) Under no ILC (July12)



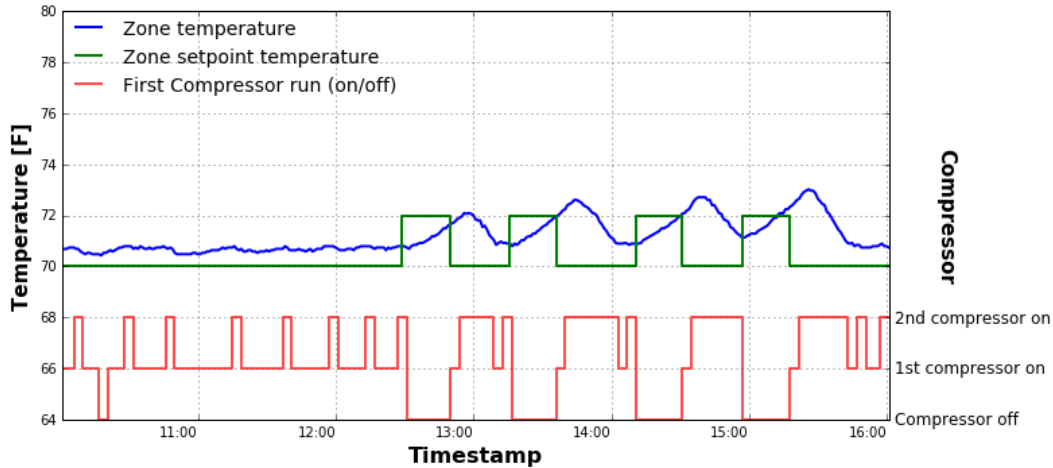
(b) Under ILC (July11)

Figure 14. Electric demand and outdoor temperature profiles during cooling season

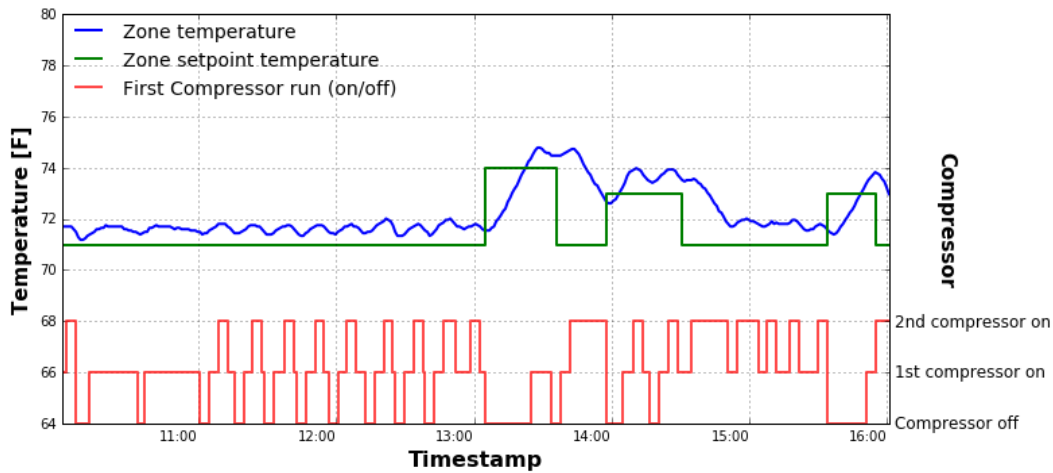
Figure 15 shows the temperature and stage profiles under ILC. Both heat pumps have two separate compressor circuits. Output stages of heat pump systems shown on the second y-axis indicate the first and second compressors of heat pumps, respectively. The OFF state is denoted by 0 in the figures. As recommended by the building operator, the offset value of each heat pump was determined to be higher than 3°F. For example, the set point offset was set to 2°F for HP-6 and 3°F for HP-4 lower than the normal set point. When the ILC event ended, the set points returned to their original values.

As shown in Figure 15a, the zone temperature of HP-6 increased less than 1°F compared to the one before compressors were turned OFF during all ILC events. The first compressor was subsequently turned OFF after the second compressor was turned OFF. Under ILC, no compressor was turned ON, which means zone temperatures did not increase significantly.

As shown in Figure 15b, ILC resulted in a zone temperature increase when HP-4 was curtailed to manage the peak demand level. For example, during the first ILC event, the maximum deviation of zone temperatures from the normal set point was 3.5°F. In this case, HP-4 started running in cooling operation mode because the zone temperature was higher than the offset set point. This prevented any possible occupant discomfort during ILC. When this happens, another heat pump is triggered to be OFF to avoid exceeding the target peak demand. Overall, ILC successfully dropped demand in the applicable spaces to meet the established limit while sustaining occupant comfort levels.



(a) HP-6



(b) HP-4

Figure 15. Example of temperature and heat pump stage profiles the at the test building during ILC

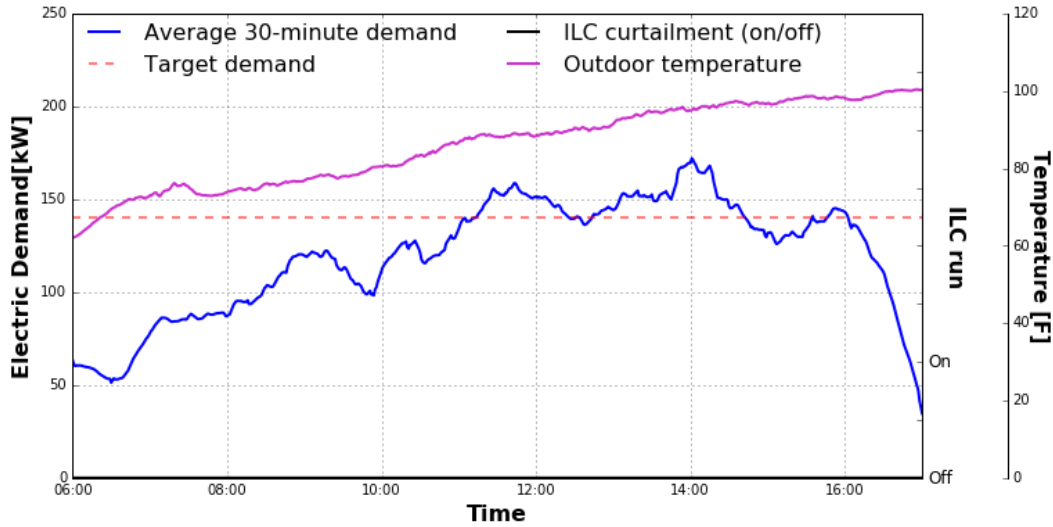
Table 17 shows the summary of curtailment of each heat pump during ILC on July 11. The symbol O indicates that ILC curtailed the unit to an OFF state. There were five ILC events while HP-3, HP-4, HP-6, and HP-7 were switched in turn. The heat pumps serving the kitchen and shops were mainly selected. Because all shops were open spaces, the heat pumps were running at all times (e.g., HP-5 and HP-8), which prevented the zone temperature from increasing significantly.

Table 17. Summary of curtailment of each heat pump for the cooling case study

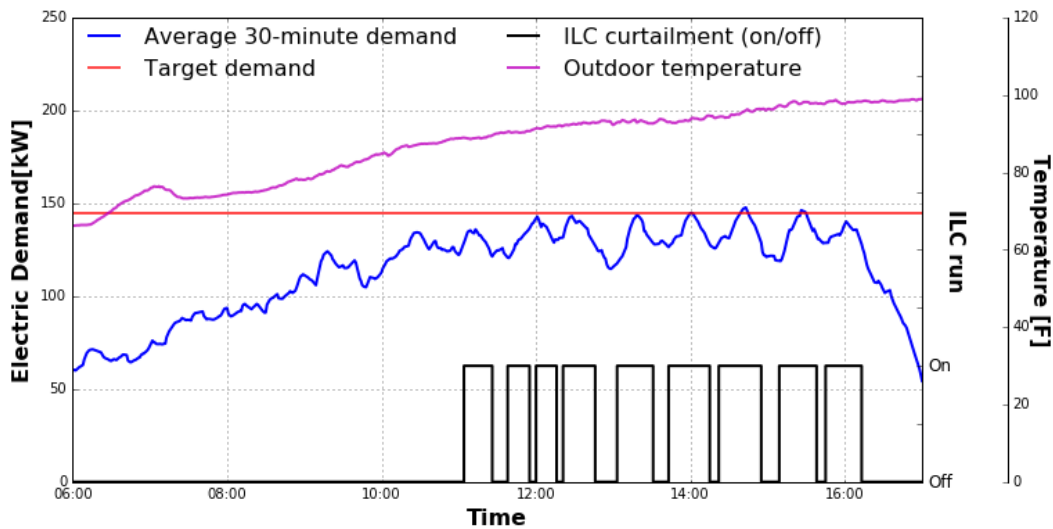
System Model	Room Type	Capacity [tons]	1 st ILC	2 nd ILC	3 rd ILC	4 th ILC	5 th ILC	Number of Curtailments
HP1-A	Manager Office	2						0
HP1-B	Office	2						0
HP-2	Manager Office	2						0
HP-3	Kitchen	7.5	O				O	2
HP-4	Shop	7.5		O	O		O	3
HP-5	Shop	4						0
HP-6	Shop	25	O	O	O	O		4
HP-7	Office	7.5			O	O	O	3
HP-8	Shop	20						0
HP-350	Office	3						0
Total Heat Pump Curtailments			2	2	3	2	3	12

7.1.3 Demonstration Results for ILC during the Cooling Season (August)

To demonstrate the capabilities of ILC algorithm under similar outdoor temperatures, 2 days with temperatures over 100°F were selected: August 5 and August 16, as shown in Figure 16. Figure 16a shows the maximum peak demand as 175 kW at 2 p.m. when the outdoor temperature was 96°F. Figure 16b shows the demand profile under ILC. Although target peak demand under such high outdoor temperatures should have been increased based on the WBE method, the demonstration used the aggressive target peak demand of 140 kW for consistency. As shown in Figure 16b, ILC was run for extended hours from 11 a.m. to 4 p.m. with nine ILC events. Overall, the ILC algorithm can maintain demand at the target peak level.



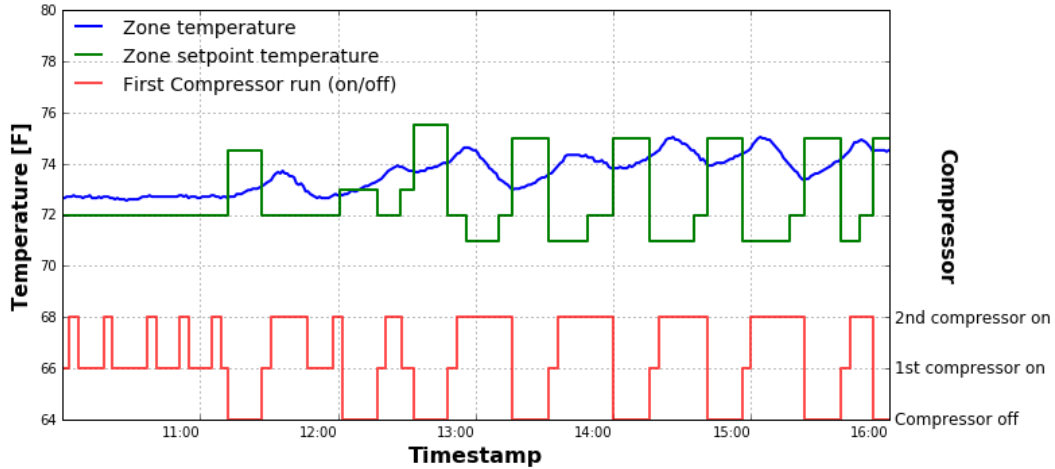
(a) Under no ILC (August5)



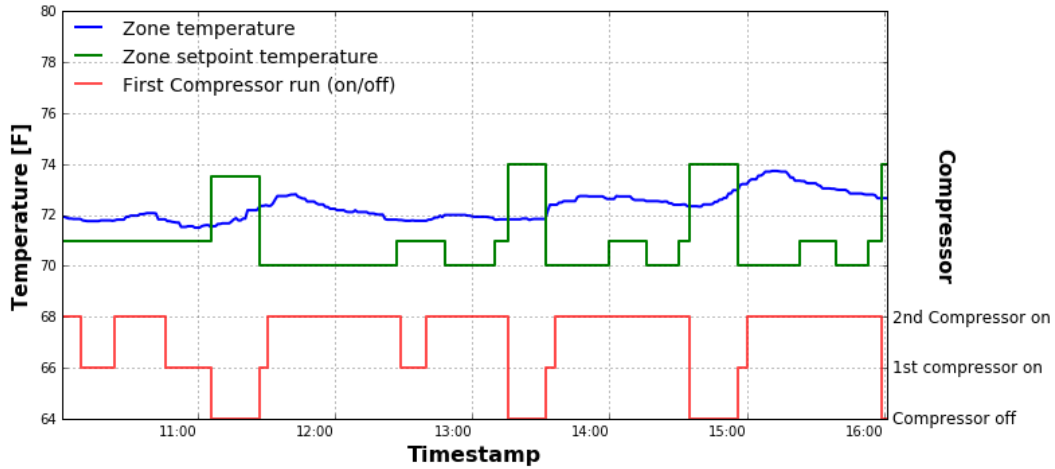
(b) Under ILC (August16)

Figure 16. Electric demand and outdoor temperature profiles during cooling season at the test building

Figure 17 shows example temperature and heat pump status signal profiles under ILC on August 16. To accommodate the aggressive target peak demand, the offset set point was changed from 3°F to 4°F. During the ILC test, according to the building operators they did not receive any complaints from occupants. The set point of HP-6 increased by 1°F from the original set point during each ILC event. Although the zone temperature was increased by 4°F due to the aggressive target demand level after all ILC events ended, the increase was not significant enough to cause occupant discomfort. As shown in Figure 17b, the difference between the original set point and zone temperature of HP-4 was less than 3°F, thus sustaining the comfort level. Only one of three attempts to turn OFF the second stage compressor was successful because the deviation between offset set point and zone temperature was significant enough to keep the compressor ON.



(a) HP-6



(b) HP-4

Figure 17. Temperature and heat pump status signal profiles at the test building during ILC

Table 18 shows the summary of curtailment of each heat pump during ILC on August 16. Because of the aggressive target peak demand, there were nine ILC events, which are significantly more frequent than other test cases. While HP-3, HP-4, HP-6, and HP-7 were mainly switched OFF, HP-2 and HP-8 were also turned ON and OFF to reduce the peak demand. For the seventh ILC event in particular, 85% of the total capacity of heating, ventilation, and air-conditioning was curtailed. When the zone temperature was higher than the offset set point, the corresponding heat pumps were turned ON and thus the comfort level was not jeopardized.

Table 18. Summary of curtailment of each heat pump for the cooling case study

System Model	Room Type	Capacity [tons]	1 st ILC	2 nd ILC	3 rd ILC	4 th ILC	5 th ILC	6 th ILC	7 th ILC	8 th ILC	9 th ILC	Number of Curtailments
HP1-A	Manager Office	2										0
HP1-B	Office	2										0
HP-2	Manager Office	2				0			0			2
HP-3	Kitchen	7.5	0			0	0	0	0	0	0	7
HP-4	Shop	7.5	0			0	0	0	0	0	0	7
HP-5	Shop	4										0
HP-6	Shop	25	0		0	0	0	0	0	0	0	8
HP-7	Office	7.5		0		0	0	0	0	0	0	7
HP-8	Shop	20							0			1
HP-350	Office											0
Total Heat Pump Curtailments			3	1	1	5	4	4	6	4	4	32

8.0 Conclusions

The overall goal of this work was to develop, validate and demonstrate that ILC algorithm can be deployed to manage building peak consumption. The ILC process uses the AHP to dynamically prioritize the available controllable loads for curtailment in a building or a group of buildings. The ILC process can be implemented on low-cost hardware (e.g., Beagle Bone, Raspberry PI, Intel NUC, etc.) on a supervisory controller without the need for additional sensing. First, the ILC process was tested in a simulation environment to control a group of RTUs to manage a building's peak demand. The test showed that the peak load can be reduced while still maintaining the zone temperatures to within acceptable deviations. We describe the process as parameter-light because only a few input variables need to be set by the user. The key parameters include the curtailment time period and target peak demand level. Based on the virtual test bed results, we discussed the influence of the parameters choices and provided guidance to setting initial parameter for the ILC.

The ILC agent using VOLTTRON was implemented and demonstrated to manage the electric demand in the test building on the PNNL campus. The ILC using target levels estimated by WBE was tested under different outdoor operating conditions. Based on the test results, the ILC was successful in coordinating how many RTUs run concurrently, thereby maintaining the building peak demand to the target level without a significant reduction in occupant comfort.

By anticipating future demand, the process can be extended to add advanced control features such as precooling and preheating to alleviate comfort issues when the RTUs are curtailed to manage the peak demand. Although the ILC process described and validated in this report was highly tailored to work with RTUs, it can be generalized and applied to any controllable loads in a building, such as those of variable air volume boxes and lighting. Furthermore, the ILC process can be extended to manage building loads based on an energy budget instead of peak consumption.

9.0 References

- Aalami H, MP Moghaddam, and GR Yousefi. 2010. Modeling and prioritizing demand response programs in power markets. *Electric Power Systems Research* 80(4), 426–435.
- Bian D, M Pipattanasomporn and S Rahman. 2015. A Human Expert-Based Approach to Electric Peak Demand Management. *IEEE Trans. Power deliver* 30(3), 1119–1127.
- Cheng EWL, and H Li. 2002. Construction partnering process and associated critical success factors: quantitative investigation. *Journal of Management in Engineering* 18(4), 194–202.
- Crowe TJ, and JS Noble. 1998. Multi-attribute analysis of ISO 9000 registration using AHP. *International Journal of Quality and Reliability Management* 15(2), 205–22.
- Ding Z, S Srivastava and D Cartes. 2006. Expert system based dynamic load shedding scheme for shipboard power systems. *In Industry Applications Conference, Oct. 2006, 41st IAS Annual Meeting Conference Record of the 2006 IEEE*, 3(2), 1338–1344.
- Goh, HH, and BC Kok. 2010. Application of Analytic Hierarchy Process (AHP) in load shedding scheme for electric power system. *In International Conference Environment and Electric Engineering, May 2010. 9th International Conference*, 365–368.
- Hoffman AJ. 1998. Peak demand control in commercial buildings with target peak adjustment based on load forecasting. *In Control Applications, Proceedings of the 1998 IEEE International Conference, Vol. 2*, 1292–1296.
- Katipamula S, MR Brambley, and J Schein. 2003. Energy Efficient and Affordable Small Commercial and Residential Buildings Research Program -- Project 2.7 – Enabling Tools, Task 2.7.4 –Results of Testing WBD Features under Controlled Conditions. Battelle – Pacific Northwest Division, Richland, Washington.
- Kim D, JE Braun, E Cliff, and J Borggaard. 2014. Development of control benefit evaluation tool for small commercial buildings. ASHRAE/IBPSA-USA Building Simulation Conference.
- Kim D, JE Braun, E Cliff and J Borggaard. 2015. Development, Validation and Application of a Coupled Reduced-order CFD model for Building Control Applications. *Building and Environment* 93(2), 97–111.
- Krarti M. 2000, *Energy Audit of Building Systems: An Engineering Approach*. CRC Press, Boca Raton, London/New York.
- Lee KH, and JE Braun. 2008. Model-based demand-limiting control of building thermal mass. *Building and Environment* 43(10), 1633–1646.
- Lu N, and S Katipamula. 2005. Control strategies of thermostatically controlled appliances in a competitive electricity market. *In Proceedings of Power Engineering Society General Meeting, June 2005, IEEE 1*, 202–207.
- Saaty TL. 2003. Decision-making with the AHP: Why is the principal eigenvector necessary? *European Journal of Operational Research* 145(1), 85–91.

Saaty TL and LG Vargas. 2012. Models, Methods, Concepts and Applications of the Analytic Hierarchy Process, Vol. 175. Springer Science & Business Media.

Taylor JW. 2003. Short-term electricity demand forecasting using double seasonal exponential smoothing. *Journal of Operational Research Society* 54, 799–805.

Thumann A, and DP Mehta. 2001. Handbook of Energy Engineering. The Fairmont Press, Inc.

Triantaphyllou E and HM Stuart. 1995. Using the analytic hierarchy process for decision making in engineering applications: some challenges, *International Journal of Industrial Engineering: Applications and Practice* 2(1), 35–44.

Yao Y, Z Lian, S Liu and Z Hou. 2004. Hourly cooling load prediction by a combined forecasting model based on analytic hierarchy process. *International Journal of Thermal Sciences* 43(11), 1107–1118.

Wong JK and H Li. 2008. Application of the analytic hierarchy process in multi-criteria analysis of the selection of intelligent building systems. *Building and Environment* 43(1), 108–125.